



VILNIUS GEDIMINAS TECHNICAL UNIVERSITY
FACULTY OF CIVIL ENGINEERING
DEPARTMENT OF BUILDING MATERIALS

Romualdas Randamanskas

**STIFFNESS INFLUENCE INVESTIGATION IN PLAIN AND BRANCHED
TIMBER USING NON-DESTRUCTIVE METHOD**

**ŠAKOTOS MEDIENOS TAMPRUMO RODIKLIŲ NUSTATYMAS
NEARDOMUOJU METODU**

Master's thesis

Building Materials and Products study program, study code 621J82001

Building Technology fields of study

Vilnius, 2015



VILNIAUS GEDIMINO TECHNIKOS UNIVERSITETAS

STATYBOS FAKULTETAS

STATYBINIŲ MEDŽIAGŲ KATEDRA

Romualdas Randamanskas

**ŠAKOTOS MEDIENOS TAMPRUMO RODIKLIŲ NUSTATYMAS
NEARDOMUOJU METODU**

**STIFFNESS INFLUENCE INVESTIGATION IN PLAIN AND BRANCHED
TIMBER USING NON-DESTRUCTIVE METHOD**

Baigiamasis magistro darbas

Statybos medžiagos ir dirbiniai studijų programa, valstybinis kodas 621J82001

Statybų technologijų studijų kryptis

Vilnius, 2015

VILNIUS GEDIMINAS TECHNICAL UNIVERSITY
FACULTY OF CIVIL ENGINEERING
DEPARTMENT OF BUILDING MATERIALS

APPROVED
Head of Department

(Signature)

Gintautas Skripkiūnas

(Name, Surname)

2015.06.01

(Date)

(Date)

Romualdas Randamanskas

**STIFFNESS INFLUENCE INVESTIGATION IN PLAIN AND BRANCHED
TIMBER USING NON-DESTRUCTIVE METHOD**

**ŠAKOTOS MEDIENOS TAMPRUMO RODIKLIŲ NUSTATYMAS
NEARDOMUOJU METODU**

Master's thesis

Building Materials and Products study program, study code 621J82001

Building Technology fields of study

Academic Supervisor

(Degree, name, surname)

(Signature)

(Date)

Vilnius, 2015

VILNIAUS GEDIMINO TECHNIKOS UNIVERSITETAS

STATYBOS FAKULTETAS

STATYBINIŲ MEDŽIAGŲ KATEDRA

APPROVED
Head of Department

(Signature)

Gintautas Skripkiūnas

(Name, Surname)

2015.06.01

(Date)

Romualdas Randamanskas

**ŠAKOTOS MEDIENOS TAMPRUMO RODIKLIŲ NUSTATYMAS
NEARDOMUOJU METODU**

**STIFFNESS INFLUENCE INVESTIGATION IN PLAIN AND BRANCHED
TIMBER USING NON-DESTRUCTIVE METHOD**

Baigiamasis magistro darbas

Statybos medžiagos ir dirbiniai studijų programa, valstybinis kodas 621J82001

Statybų technologijų studijų kryptis

Vadovas

(Moksl. laipsnis/pedag. vardas, pavardė)

(Parašas)

(Data)

Vilnius, 2015

VILNIUS GEDIMINAS TECHNICAL UNIVERSITY
FACULTY OF CIVIL ENGINEERING
DEPARTMENT OF BUILDING MATERIALS

Building Technology fields of study

Building Materials and Products study program, study code

621J82001

APPROVED
Head of Department

(Signature)

Gintautas Skripkiūnas

(Name, Surname)

2014.10.15

(Date)

MASTER'S THESIS TASK

No.

Vilnius

Student Romualdas Randamanskas

(Name, Surname)

Master's thesis title: **Stiffness Influence Investigation In Plain And Branched Timber Using Non – Destructive Method**

Deadline of master's thesis: June 3, 2015.

MASTER'S THESIS TASK:

Introduction;

Wood structure;

Elastic properties;

Mathematical calculation model;

Variety and nature of fundamental sound wave;

Wave propagation in solid and porous material;

Experimental part;

Conclusions;

Reference list.

Academic Supervisor

(Signature)

(Degree, name, surname)

Task obtained

(Signature)

(Name, Surname)

2014.10.14

(Date)

VILNIAUS GEDIMINO TECHNIKOS UNIVERSITETAS
STATYBOS FAKULTETAS
STATYBINIŲ MEDŽIAGŲ KATEDRA

Statybų technologijos studijų kryptis

TVIRTINU
Katedros vedėjas

Statybos medžiagos ir dirbiniai studijų programa, valstybinis
kodas 621J82001

(Parašas)
Gintautas Skripkiūnas

(Vardas, Pavardė)
2014.10.15

(Data)

**BAIGIAMOJO MAGISTRO DARBO
UŽDUOTIS**

Nr.

Vilnius

Studentui (ei) Romualdas Randamanskas

(Vardas, pavardė)

Baigiamojo darbo tema: **Šakotos medienos tamprumo rodiklių nustatymas nardomuoju metodu**

Baigiamojo darbo užbaigimo terminas 2015 m. birželio 03 d.

BAIGIAMOJO DARBO UŽDUOTIS:

Įvadas;

Medžio struktūra;

Elastinės savybės;

Matematinis skaičiavimo modelis;

Garso bangų įvairovė ir prigimtis;

Bangos sklidimas kieta ir porėta medžiaga;

Tiriamoji dalis;

Rezultatai;

Išvados;

Literatūros sąrašas.

Vadovas

(Parašas)

(Moksl. laipsnis/pedag.vardas, vardas, pavardė)

Užduotį gavau

(Parašas)

(Vardas, pavardė)

2014.10.14

(Data)

Vilniaus Gedimino technikos universitetas

Statybos fakultetas

Statybinių medžiagų katedra

ISBN ISSN

Egz. sk.

Statybos studijų programos baigiamasis magistro darbas

Pavadinimas **Šakotos medienos tamprumo rodiklių nustatymas neardomuoju būdu**

Autorius **Romualdas Randamanskas**

Vadovas prof. dr. **Albinas Gailius**

Kalba

anglų

Anotacija

Medis - viena populiariausių statybinių medžiagų, naudojamų iki šių dienų. Statybose medis aptinkamas tiek statant, tiek ir rengiant vidaus apdailą. Statybose naudojama konstrukcinė mediena yra parenkama atsižvelgiant į statybos reglamentuose, ją sugraduojant pagal nurodytas mechanines savybes, fizikinę išvaizdą, drėgnumą ir esamus defektus. Dažniausiai pasitaikantys medienos defektai yra įaugusios šakos, įtrūkiai, puviniai ir apdirbimo pažaidos.

Šiame baigiamajame magistro darbe buvo tiriamas dažniausiai pasitaikantis defektas - įaugusi šaka. Medienos gaminio šakotumas yra skirstomas pagal kiekį, dydį, paviršiaus plotą ir gylį, yra atsižvelgiama, ar šaka yra įaugusi, ar iškritusi. Šakotumas lemia medienos mechanines savybes. Medienos gaminiuose įaugusi šaka identifikuojama kaip tamsi, apvali dėmė, kuri skiriasi tankiu ir struktūra. Augant medžiui, šaka auga iš kamieno ir yra pasvirusi iki 90 laipsnių vertikaleje. Atsitinka, kad medžio augimo metu, šaka yra nupjaunama ir toliau augant medžiui jos dalys lieka kamieno viduje. Klasifikuojant tokius medžio gaminius, toks defektas yra traktuojama kaip skylė.

Vienas pagrindinių tiriamojo darbo tikslų yra pateikti norvegiškos eglės (*Picea abies(L.) Karst*) sveikos ir šakotos medienos bandinių struktūros skirtumus fizikiniu ir mechaniniu požiūriu. Tiriamojo darbo rezultatai rodantys tamprumo pasiskirstymą bus pateikiami grafiškai, apibendrinami išvadomis. Tiriamajame darbe rezultatai pateikti grafiškai parodant, kaip įaugusios šakos vieta keičia mechanines ir fizikines savybes.

Vienas iš pagrindinių baigiamojo darbo uždavinių yra nustatyti vientisos ir šakotos medienos tamprumą naudojant neardomąjį metodą, tiriant bandinius ultragarsu. Metodas yra taikomas įvairioms medžiagoms tiek tankioms, tiek porėtoms - tirti. Didelis pranašumas yra tas, kad atliekant tyrimus nereikia mechaninio apdorojimo, bandinius užtenka paveikti garso bangomis naudojant specialią įrangą. Remiantis naujausiais moksliniais tyrimais, tiriamojo darbo metodika ir garso bangų parametrai yra nagrinėjami literatūros apžvalgoje.

Darbą sudaro 9 dalys: įvadas, medžio struktūra, elastingos savybės, matematinis skaičiavimo modelis, garso bangų įvairovė ir prigimtis, bangos sklidimas kieta ir porėta medžiaga, tiriamoji dalis, rezultatai, išvados, literatūros sąrašas.

Darbo apimtis – 81 p. teksto be priedų, 40 iliustr., 5 lent., 77 bibliografiniai šaltiniai.

Prasminiai žodžiai: medis, norvegiškoji eglė, anizotropinės, garso bangos, neardomasis metodas, tamprumo matrica.

Vilnius Gediminas Technical University
Civil engineering faculty
Building Materials department

ISBN ISSN
Copies No.
Date-....-....

Building Materials and Products study programme master's thesis.

Title: **Stiffness Influence Investigation in Plain and Branched Timber Using Non-Destructive Method**

Author **Romualdas Randamanskas** Academic supervisor prof. dr. **Albinas Gailius**

Thesis language
English

Annotation

Tree - one of the most popular building materials used today. In civil engineering timber found in dwellings construction and in the development of house interior. Structural wood used in construction is selected according to building regulations by the mechanical properties, physical appearance, moisture content and existing defects. The most common wood defects are branches, cracks, rots and damage caused by processing.

In this master's thesis will be tested the most common defect - rooted branch. In wood products knots are classified by quantity, size, surface area and depth. Branched places of timber determines the mechanical properties of wood. Rooted branch is identified as a dark, round spot, which is different in density and structure. During tree growing period branches are inclined up 90 degrees to the vertical. It happens that during tree growth period the branch is cut and the tree continues to grow as its parts remain inside the trunk. Classifying such defect is treated as a hole in the timber.

One of the main objectives of the research work is to present Norwegian spruce (*Picea abies* (L.) Karst) how plain and branched timber differences operate in physical and mechanical scales. The results of the investigation will show distribution of the elasticity. Research project results will be presented graphically showing how branch changes mechanical and physical properties of plain wood.

One of the main objectives of the thesis is to find a plain and branched wood elasticity using a non-destructive method. The method is applicable investigating various materials both solid and porous. Big advantage that experiment does not require mechanical processing, samples are affected by sound waves using special equipment. Sound waves parameters are considered in the literature review according to recent scientific publications, research work and various methodologies.

The work consists of 9 parts: introduction, wood structure, elastic properties, mathematical calculation model, variety and nature of fundamental sound wave, wave propagation in solid and porous material, experimental part, conclusions and references.

Work size - 81 p. text without appendixes, 40 illustrations, 5 tables, 77 bibliographic sources.

Keywords: Tree, wood, timber, Norwegian spruce, anisotropic materials, ultrasound, non – destructive method, elasticity matrix.

The document of Declaration of Authorship in the Final Degree Project

VILNIUS GEDIMINAS TECHNICAL UNIVERSITY

Romualdas Randamanskas 20094328

(Student's given name, family name, certificate number)

Faculty of Civil Engineering

(Faculty)

Construction Material and Products

(Study programme, academic group no.)

**DECLARATION OF AUTHORSHIP
IN THE FINAL DEGREE PROJECT**

(Date)

I declare that my Final Degree Project entitled "STIFFNESS INFLUENCE INVESTIGATION IN PLAIN AND BRACHED TIMBER USING NON-DESTRUCTIVE METHODS" is entirely my own work. The title was confirmed on _____ by Faculty Dean's order

(Date)

No. _____. I have clearly signalled the presence of quoted or paraphrased material and referenced all sources.

I have acknowledged appropriately any assistance I have received by the following professionals/advisers: _____

The academic supervisor of my Final Degree Project is prof. dr. Albinas Gailius .

No contribution of any other person was obtained, nor did I buy my Final Degree Project.

(Signature)

(Given name, family name)

1. Content

1.	Content.....	10
1.1	List of Figures	11
1.2	List of Tables.....	12
2.	Abstract	13
2.1.	Introduction.....	14
2.2.	Tasks	15
2.3.	Objectives	15
2.4.	Scope of work	16
3.	Wood structure.....	17
3.1.	General Wood structure	17
3.2.	Wood cell composition	19
3.3.	Multiscale micromechanical model	20
3.4.	Wood cell morphology	22
3.5.	Wood cell size and topology.....	24
3.6.	Wood Knots	24
4.	Elastic Properties	26
4.1.	Modulus of elasticity	27
4.2	Shear modulus	28
4.3	Poisson's Ratio	30
5.	Mathematical Description of Stiffness Derivation for Orthotropic Materials.....	31
5.1.	Elastic symmetry	34
5.2.	Elastic Wave Propagation in Anisotropic Media	39
5.3.	Elastic waves	40
6.	Variety and nature of fundamental sound wave	44
6.1.	Wave propagation in solid and porous materials.....	44
6.1.1.	P-waves.....	45
6.1.2.	S-waves.....	46

6.1.3. Rayleigh waves	48
6.1.4. Lamb waves	49
6.1.5. Bulk waves.....	50
7. Experimental Part	51
7.1. Non-Destructive Testing with Ultrasound Equipment	51
7.2. Samples	55
7.3. Marking of Specimens	58
7.4. Measuring of specimens	59
7.5. Results.....	62
8. Conclusions.....	72
9. References list.....	74

1.1 List of Figures

Figure 3.1: Cross-section of a young conifer stem showing wood structure. (From Fritts, 1979) (18 p.)

Figure 3.2: Wood cell. After T.L. Rost et al (1979): Botany, a brief introduction to plant biology (21 p.)

Figure 3.3: Ultrastructural organisation of cellulose microfibrils, hemicellulose and lignin within the wood cell wall and (b) schematic illustration of the cell wall of a softwood tracheid with different orientation of cellulose microfibrils in the layers (Fengel, 1969) (22 p.)

Figure 3.4: Two types of knots encountered in wood grading. Loose knots on the left often fall out as the wood dries. Tight knots such as the one on the right are coalesced with wood but need sealing. (Meredith, 2015) (25 p.)

Figure 6.1: Wavefronts and raypaths for the wave propagating from a source. (44 p.)

Figure 6.2: Perspective view of elastic P-wave propagation through a grid representing a volume of material (45 p.)

Figure 6.3: Perspective view of elastic S-wave propagation through a grid representing a volume of material (47 p.)

Figure 6.4: Perspective view of Rayleigh-wave propagation through a grid representing a volume of elastic material. (48 p.)

Figure 6.5: Lamb wave propagating in plate: (a) symmetric; (b) antisymmetric (49 p.)

Figure 6.6: Schematic diagram showing (from left to right) pure bulk wave propagation modes with longitudinal, shear-vertical and shear-horizontal polarization. (51 p.)

Figure 7.1: Ultrasonic Signal Preamplifier (5676), Panametrics Inc., Waltham, MA, USA) (52 p.)

Figure 7.2: Longitudinal Transducers (53 p.)

Figure 7.3: Transversal Transducers (53 p.)

Figure 7.4: Delay line (53 p.)

Figure 7.5: Correction time with longitudinal transducers (54 p.)

Figure 7.6: Correction time with transversal transducers (55 p.)

Figure 7.7: Coupling agent (honey) is smeared over entire surface of transducers and covered with plastic film (55 p.)

Figure 7.8: Picture of the first sample (56 p.)

Figure 7.9: Picture of the second sample (57 p.)

Figure 7.10: First sample specimens marking (58 p.)

Figure 7.11: Second sample specimens marking (59 p.)

Figure 7.12: 10 and 29 specimen from the first sample (61 p.)

Figure 7.13: Knotted specimens from second example (62 p.)

Figure 7.14: Schematical representation of geometrical coordinate system of single specimen, where blue is **X** axis with length of 10 mm, red is **Y** axis with length of 10 mm and green is **Z** axis with height of 20mm. (63 p.)

Figure 7.15: Stiffness distribution along A axis (64 p.)

Figure 7.16: Stiffness distribution along B axis (64 p.)

Figure 7.17: Stiffness distribution along C axis (65 p.)

Figure 7.18: Stiffness distribution along D axis (65 p.)

Figure 7.19: Density distribution along axis (66 p.)

Figure 7.20: Second sample longitudinal stiffness distribution along Z direction (67 p.)

Figure 7.21: Second sample longitudinal stiffness distribution along Y direction (67 p.)

Figure 7.22: Second sample longitudinal stiffness distribution along X direction (68 p.)

Figure 7.23: Second sample shear stiffness distribution along XZ direction (68 p.)

Figure 7.24: Second sample shear stiffness distribution along YZ direction (69 p.)

Figure 7.25: Second sample shear stiffness distribution along YX direction (69 p.)

Figure 7.26: Second sample shear stiffness distribution along ZX direction (70 p.)

Figure 7.27: Second sample shear stiffness distribution along XY direction (70 p.)

Figure 7.28: Second sample shear stiffness distribution along ZY direction (72 p.)

Figure 7.29: Second sample density distribution (72 p.)

1.2 List of Tables

Table 7.1: First sample average dimensions of specimen (59 p.)

Table 7.2: Second sample average dimensions of specimen (60 p.)

Table 7.3: Average physical properties of the first and second sample (60 p.)

Table 7.4: Specimen 10 and 29 physical characteristics (61 p.)

Table 7.5: Physical characteristics of second example knot (62 p.)

2. Abstract

Wood is worldwide recognized and very popular material used in building construction. Wood is worth to use in dwelling house construction. Depends from climate zone, in some regions like South America, that do not pass temperature jumps from negative to positive, wood is used for carcass, empty volumes filling with porous concrete. Still, in common practice timber boards are used for roof carcass. For works, where some external and permanent loads are expected suitable dimensions of timber element should be chosen. Structural wood is selected by certain building codes that require knowing mechanical characteristics like compressive strength and moisture resistance. In production of constructional wood every part is assigned to certain grade that selected by wood species, age and external deformations. It is determined accurately when test for physical characteristics are carried out, also grade defined by visual appearance. Considering amount of size and placement of knots, slopes of grain, manufacturing defects, waness and warps on lumber sets its grade. Nether or less, physical properties are more important than esthetic appearance. It is very important to know when certain defects imply its mechanical behavior.

A knot is the most common imperfection in the wood. It is recognized as defect of wood than can affect technical properties depending from its quantity, size and depth. Knot is formed from rooted branch that grows, up to 90 degrees different from the grain direction. During tree growing lower limbs may remain attached for certain period of years. Stems are no longer connected with the dead limb, but are overgrown around it. In lumber, knot will appear as solid, circular, usually darker spot. In constructional wood where strength is important parameter knots may weaken the timber but it depend upon their position, size, number and condition. Knot stiffness differs but do not necessarily influence the stiffness of structural timber. One of main tasks of this master thesis will be to find out how stiffness is allocated in plain and knotted timber. If knot is still grown into the grain it will give a little resistance to the tensile stress. Evaluating distribution of stiffness properties in certain regions will allow calculating mechanical behavior. After all, knowing that given results correlates with the material, calculations with increased knot distribution and specimen size will be possible

For obtaining stiffness parameters non-destructive method will be used. It can be used to obtain properties for wide range, from solids to porous materials. Evaluating by ultrasound doesn't require mechanical processing and it gives most accurate results with less error. With specialized equipment that is able to send precisely set sound wave threw the specimen that is put between transducers. Wave is set in pulser-receiver device and received results are shown with the help of oscilloscope. More in detail about non-destructive equipment wave propagation in anisotropic material will be described in experimental part.

The aim of this work is understand structure differences and physical properties of knotted and plain timber in different scales. Using non-destructive techniques evaluate and distribute stiffness parameters.

2.1. Introduction

Norway spruce (*Picea abies(L.) Karst*) is economically and ecologically one of the most important tree species all over Europe used in building industry. In sawmilling, pulping and papermaking the improvement of end-product quality and economical yield is the result of modern precision of machinery. To understand the possibilities of the wood firstly need to look into history of architecture. Wood always was material with low transportation costs, before first engines, people used rivers to transport wood as building material. Wood can be used in all building steps including scaffolding manufacturing, construction of carcass or exterior and interior decorations.

Nowadays, a lot of examples of wood applications are seen in buildings living or working spaces. People who prefer timber in the working or living area will get dry, fresh and natural atmosphere. Naturally, timber also known for its acoustic properties enables to create coziness in all the place. Using wood as building material for walls or roof you will guarantee that air in house will be ventilated. More to say, that that wood popular for its thermal properties. Wood structure is designed to change air transmission properties during temperature changes. Nowadays, gathered knowledge and experience let us to create new substitutes for the wood in building technology, still, they consume a lot of time and recourses. Not a lot of known about wooden structure parameters which allows us to get same properties material as wood is described. Its anisotropic structure leads to complex elasticity tensor matrix transformations that are computed numerically. Mathematical models that were described by Huntington 1950, Sabina and Willis 1988, Bose and Mall 1973, Data 1977 and much more, will help to find mechanical properties using ultrasound pulse. In this master thesis big attention will be given to works of Kohlhauser 2009, where ultrasonic contact pulse-transmission to determine elastic stiffness of materials are described in easily understandable way. Values will be obtained using non-destructive technique like ultrasonic pulse to enable elasticity tensor for an anisotropic materials using Kelvin- or Mandel- notation (Cowin and Mehrabadi 1992; Helnwein 2001; Cowin 2003) to obtain twelve engineering constants that include three Young's moduli, three shear moduli and six Poisson's ratios. Before starting mathematical evaluation of material, acoustical wave's properties for longitudinal and transverse transducers will be defined (look for Chapter 6).

Before using wood as building material it should be cut and evaluated by special building codes. All methodology in wood grading includes knot detection and other physical structure defects. A

knot is the most common defect in classifying timber class. Threw the detection knot diameter and depth is evaluated, physical parameters as moisture and density are also taken into account. If timber is not treated by processes of impregnation or vanishing it loses mechanical properties much faster than plain timber, taking into account that branch which was grow in the wood is mostly perpendicular to stem. Growing tree identifies branch as obstacle and do nothing more as bypasses around not sharing same water circulation system. Wooden structures are highly resistant under continuous periodical loads and knot are in most cases are cause of micro-cracks propagation. In some calculations knot are is supposed to be a hole, mostly it depends from specimen type, part of the wood from where it was taken including growth ring range and height of the stem. This master project will cover main models. They will be discussed in methodological part of this work. It is expected to understand how much knot influence in plain wood material downgrades its mechanical properties.

In this master work non-destructive testing technique using ultrasound pulse will be evaluated to characterize mechanical properties for anisotropic materials. Before starting experiment, equipment should be graded considering structure and physical parameters as moisture and specimen size. Specimens will be measured and weighted to get mass density. Specimen's dimensions are important to set wave frequency and direction of ultrasound. Tree as anisotropic materials are described by its mechanical properties in different directions: the longitudinal direction, which coincides with the direction of the layers, the tangential direction that leads around the trunk and radial, which shows the direction to the center of the trunk.

Knot and wood grain are connected by microfibrils. Microscopic images will help to define angle of microfibril in connecting parts and use it in numerical calculations. After ultrasound data collection, mathematical model will be used to process information visually. With the help of distribution graphs, conclusions will be formed to understand knot influence in plain timber.

2.2. Tasks

- According to the reliable literature examine wood structure in several scales that represent the primary roles and functions of the tree;
- Using data acquired from ultrasound experiment find the stiffness distribution in the plain and branched wood.
- Present gathered data in understandable way using graphs and plots for both experiments and formulate conclusions.

2.3. Objectives

- In literature analysis provides relevant and up to date information relating to its methodology.

- In experimental part give a brief description of provided experiments.
- Produce methodologies and mathematical rules that are used to define the stiffness parameters in anisotropic materials by ultrasonic method.
- To get a mathematical model that allows formulating stiffness matrix to calculate material's physical behavior using acquired data from ultrasound experiment.

2.4. Scope of work

This work will submit main physical and mechanical differences between plain and knotted wood using non – destructive experiment with ultrasound. Answers will be presented using graphical images and proposing conclusions in the last chapter. Before understanding how stiffness and density differs in both regions there will reviewed various literature to understand main structure of the wood in the various scales (Chapter 3). Same literature will be used to understand how authors are trying to identify structure in plain and knotted wood regions. Young and Shear modulus will be presented including Poisson's ratio (Chapter 4). Using those properties it will be possible to show mathematical stiffness matrix composition for anisotropic materials (Chapter 5).

Before starting experimental part main theoretical laws and working principles will be arranged. Firstly, with reference from trusted literature sources, types of principal fundamental wave propagation in porous materials will be formulated (Chapter 6). For wood investigation using ultrasound longitudinal and shear waves are used, but in the nature more than those two types of waves exist (Rayleigh waves, Lamb waves, Bulk waves). Next, equipment used in the experiment will be described that was used in Technical University of Wien (Chapter 7). This part also includes brief description of specimens and all preparatory stages of the experiment. Results and conclusions will be discussed in the last section (Chapter 8).

2.5. Acknowledgments

I wrote this master project with the help of and support of Institute for Mechanics of Materials and Structures at the Vienna University of Technology. Especially thank for offered research field and main guidelines to Prof. Josef Füssl. My biggest gratitude to Dr. techn Markus Lukacevic and Dr. techn Leopold Wagner for helping to understanding process of the research work and reviewing this thesis. My biggest thanks to Dr. techn. Olaf Lahayne for his help and assistance in the lab working with samples, without his support this master thesis would never saw sunlight. Thank you to my master project supervisor at home university Prof. Albinas Gailius for consulting in various questions related to investigated materials and certain formulations.

I would like to encourage cooperation between Viena Technical, Lund Technical and Vilnius Gediminas Technical universities for opening path to such wide and puzzling scientific area where are still a lot unanswered questions that will be covered in upcoming works.

3. Wood structure

Wood is a complex, fibrous, porous, inhomogeneous and orthotropic material. Its properties frequently exhibit an unusually wide range of variability with time, loading rate, temperature and moisture content. In the first chapter principal and wood structure will be analyzed. Threw the discussion all main parts of wood consistence in different scale ranges will mentioned. After that, components of wood-cell like cellulose, hemi-cellulose, lignin and rays will be analyzed. Will be explained their functions threw tree growing season. More specifically, wood is different from annual grow rings and going deep till wood-cell composition and its properties. This variability between trees is related to growth factors determined by, for example, geographic location, site quality, soil type, and availability of moisture. Collected information from various scientific researches will help to understand what properties and geometrical conditions gives to wood such affirmative parameters.

3.1. General Wood structure

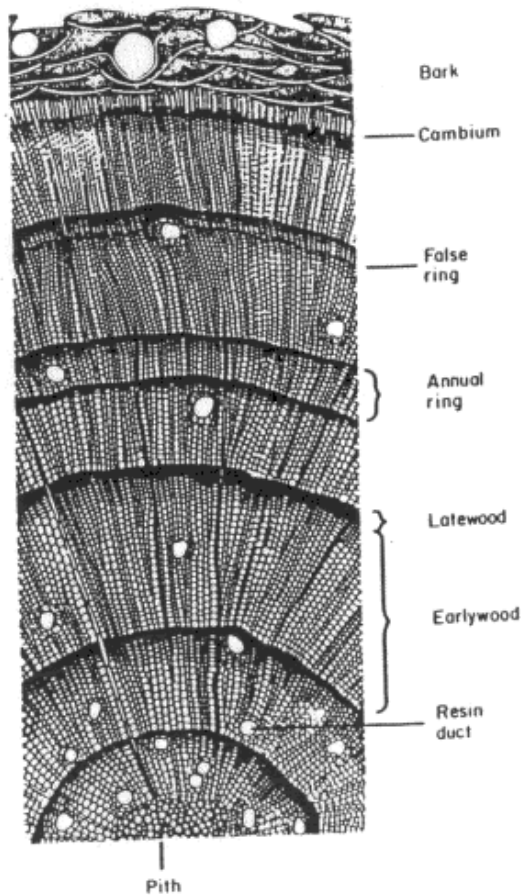


Figure 3.1: Cross-section of a young conifer stem showing wood structure. (From Fritts, 1979)

Mechanically wood can be described as a cylindrically orthotropic material with material directions according to grain parallel with longitudinal direction (Jenkel, Kaliske 2014). Wood has three mutually orthogonal twofold axes of rotational symmetry affecting material properties along each axis. To acquire such properties wood must be characterized with special geometry. Mainly, tree stem from the beginning of its growing period acquire round shape. Looking from schematic perspective it could be interpreted as circle, including various examples depending from age, temperature, air humidity and soil composition that gives errors in searching standard wood components. Still, all trees through one growing cycle creates layer in radial direction with same materials and principle structure. There will be errors in density correlation of every layer for the above mentioned reasons. In the beginning of every annual ring are possible to identify the two regions where density of timber makes visible changes. Big part

of ring's width is taken by *Earlywood* (Green *et al.*, 2002) which is created through growing cycle. In the outside part of the annual ring *Latewood* layer is observed, that is formed after growing cycle ends. It is comprised of thickly-walled, flatter cell with smaller lumen (R.D.D'Arrigo *et al.* 2000). Density difference in the annual ring is main parameter to tree-ring collection which is obtained by X-ray densitometry that results may consist annual rings with regions of low density (*Earlywood*) and high density (*Latewood*) (H. Qing, L. Mishnaevsky, 2010). This hierarchical architecture of wood is responsible for its high anisotropic and viscoelastic behavior.

Information about layer composition is used for identifying meteorological conditions. The most common source of error in tree-ring data collection is false ring formation. The main reason of false ring creation is drought in growing season causing to produce smaller-diameter, thick walled *Earlywood* cells. After drought is ended, moister conditions allow tree to return to the production of large-diameter, thick walled *Earlywood* cells (Copenheaver *et al.*, 2006). Therefore, branches and portions of the stem that are near actively growing branches are more likely to form false rings than lower, branchless sections of the stem (Fritts, 1976). Still, in this master project no special experiments

will be provided to carry out any dendrochronological purpose, but density of plain and branched timber will be evaluated. Stem exterior is protected by bark which is connected with cambium layer. Bark in older stems includes the dead tissue on the surface of the stem. (Raven, *et al*,1981), and protects inner woods from outer dangers, like parasites, temperature changes and others threats from outside.

3.2. Wood cell composition

For every tree, growing mechanics are the same. Mostly, it depends from the ratio of active substances like cellulose, hemicellulose and lignin which are main materials in developing wood-cell. They require brief explanation for what they are responsible, what are the functions and what part of wood-cell volume they take. Mainly wood is composite material made from long slender tubular cells, oriented nearly parallel of the axis of the stem and firmly connected together. Wall of cell tree major chemical constituents: cellulose (representing the fiber), hemicellulose and lignin (representing the matrix). Cellulose is encountered in a proportion of 40–50% in weight of wood substance, 25% hemicellulose and 20–30% lignin, approximately (Smith *et al*. 2003).

The cellulose is a long polymer organized into periodic crystalline and amorphous regions along its length and called crystalline–amorphous cellulose core. The length of the cellulose segment is 10,3Å. Each crystalline cellulose unit contains two segments of cellobiose and is 8,35x7,9 Å in section. The average cellulosic chain length is 50×10^3 Å (Flores *et al*. 2012).

Only non-crystalline fraction, that are made from low-molecular-weight polysaccharides, consisting of approximately 50-400 sugar units, may absorb moisture and consequently change its mechanical properties. Contrary to crystalline cellulose, hemicellulose is a polymer with little strength, built up of sugar inserts. Its structure is partially random, with mechanical properties highly sensitive to moisture changes, softening with increasing water content. The cellulosic macromolecules aggregate during biosynthesis to form crystals. The oriented cellulose chains of about 600 Å in length, with lateral dimensions of 100x40 Å, are called crystallites. The crystallites comes with relatively short amorphous regions (Green *et al*.,2002).

Lignin is an amorphous polymer that contributes as matrix to connect individual cells together and to provide shear strength. Intramolecular covalent bonds and intermolecular van der Waals forces determine a specific arrangement of cellulosic crystals, embedded in an amorphous lignin matrix. It is the most hydrophobic component in the cell-wall changes, with relatively stable mechanical properties under moisture. Aggregates of fibrils from micro fibrils, with a diameter of 200

Å, containing approximately 20 micellar strands. The width of these units is about 250 Å (de Borst *et al* 2011).

These three main constituents, cellulose, hemicellulose and lignin, form a complex network characterized by cellulose acting as a fiber embedded in a matrix composed of hemicellulose and lignin. The anisotropy at this scale is related to the disposition of cells. The wood substance is also anisotropic down to the finest detail of its crystallographic and molecular elements. This structure showed behavior of *velcro*-like plastic response similar to crystallographic sliding in polycrystalline materials (Flores *et al.* 2010). No density effects are observed at this scale because of the almost equal mass densities of cell wall materials across all wood species. However, the chemical composition changes slightly between various tree species (de Borst *et al* 2011).

3.3. Multiscale micromechanical model

Following the characteristic length scales, wood can be usually described in four different structural levels (Mishnaevsky and Qing, 2008), that will put basis for homogenization stages. To begin from the macroscale, it contains many annual rings, which appear as alternating light and dark rings. The lighter rings are called *Earlywood*, characterized by cells with large diameters and thin cell walls, while the darker rings being latewood characterized by cells with small diameters and greatly thickened cell walls and is called *Latewood*, (H. Qing, L. Mishnaevsky, 2010) data obtained from rings setting number of rings and volumetric parameters are widely usable in metrology and dendrochronology. At the mesoscale, it is a cellular material, built up by hexagon-shaped-tube cells oriented fairly parallel to the stem direction. The variability at the microscopic scale between species depends upon the relative proportion and distribution of different types of cells. The cells are differs in character; cell walls are differs in chemical composition and in organization at the molecular level. The morphological variability of cells within a tree is determined by the influence of crown elongation and cambium activity.

In some articles presence of wooden rays are mentioned that should be included into mesoscale. Ray cells might be beneficial for the tissue stiffness in tangential direction, due to a comparably higher density of the longitudinal tissue in between the rays at the same overall density. Moreover, the arrangement of the rays plays a critical role there: large ray cell bundles act as obstacles for load transfer and, thus, reduce stiffness in tangential direction. Wood can contain a considerable amount of ray cells. The most comprehensive investigation of their mechanical function was carried out by Burgert *et al.* 2001. He examined correlations between radial and tangential elastic moduli, obtained from quasistatic tension tests, with the mass density of the tissue and the volume fraction of the ray

cells. Further backed up by simple modeling based on mixture rules, he concluded mechanical relevance of rays for radial stiffness, though it was found only mass density important for tangential stiffness.

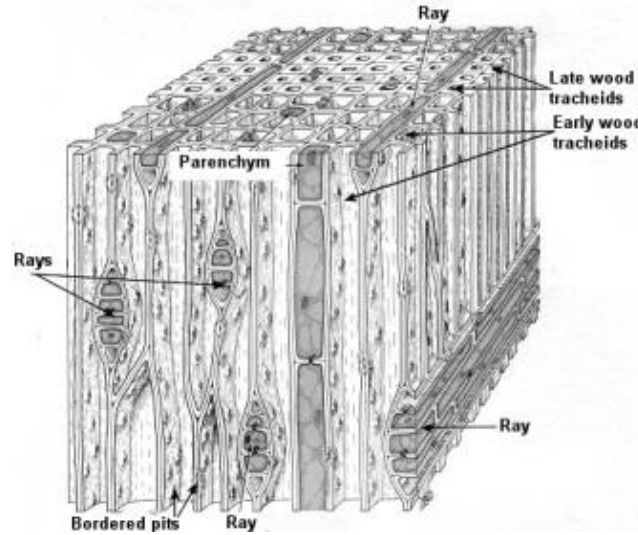


Figure 3.2: Wood cell. After T.L. Rost et al (1979): Botany, a brief introduction to plant biology

As the system increases in complexity, the microfibrils aggregate in macrofibrils. The macrofibrils are the basic building blocks of lamellae, which make up the various layers of the cell wall. The lamellae have the following generally accepted denomination (Mark 1967; Kollmann and Côté 1968; Siau 1971) of the cell wall of wood consists of 4 layers with different microstructures and properties, which are called usually P, S1, S2 and S3, and middle layer acts as bonding material. At the nanoscale, the S1, S2 and S3 layers in the secondary wall of a tracheid cell are built of several hundred individual lamellae with varied volume fractions and characteristic microfibril angles (MFA). Within each lamella the microfibrils are arranged in a typical parallel pattern and inclined with respect to the axis of the cells. This corresponds generally to the vertical growth direction of the tree.

In wood cell (Fig 3) mentioned before there are primary layer P, and three secondary layers, S1, S2 and S3 (Timell, 1986). Each layer is composed of cellulose crystalline fibrils as a framework, oriented at a different angle with reference to the cell's long axis, and embedded in isotropic hemicellulose–lignin skeleton as a matrix. The S1 layer is the thinnest of all S layers and it is hardly detectable under light microscope. The S1 layer is only 0.1–0.35mm thick and the cellulose microfibrils are oriented at a large angle toward the long axis of the tracheids (Barnett et al., 1997; Plomion et al., 2001). It represents 75–85% of the total thickness of the tracheids cell wall. The specific

orientation of microfibrils with respect to the longitudinal cell axis is microfibril angle (MFA) and is one of the most important parameters controlling the balance between stiffness and flexibility in trees (Flores *et al.*, 2010). The microfibril angle (MFA) in this layer is small, 5° – 30° to the cell long axis and the thickness fluctuates between 1 and 10mm. MFA varies with cambial age, growth rate, and height within the stem of a conifer tree and is under genetic control (Donaldson, 1992; Cave and Walker, 1994). The S3 layer is relatively thin, being 0.5–1.10mm thick and cellulose microfibrils are ordered in a parallel arrangement, but less strictly in comparison to the S2 layer, their angle is 60° – $m90^{\circ}$ towards the cell long axis (Lindstrom *et al.*, 1998).

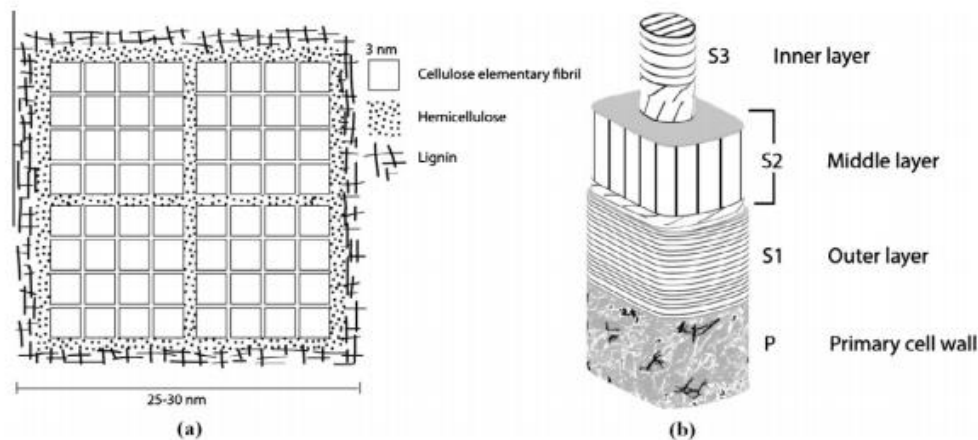


Figure 3.3: Ultrastructural organisation of cellulose microfibrils, hemicellulose and lignin within the wood cell wall and (b) schematic illustration of the cell wall of a softwood tracheid with different orientation of cellulose microfibrils in the layers (Fengel, 1969)

Sometimes microfibrils are called constituents form a spatial arrangement (Dinwoodie, 1981). Some researched were made to find out relation between microfibril angle and elastic properties of wood. By experiments which were provided with Nanoindentation technique was clear that it is no direct relation between indentation modulus and elastic modulus in longitudinal direction but the indentation modulus is strongly affected by the angle between indentation direction and microfibril orientation (A. Jäger *et al.*, 2011). Microfibrils connect inner layers of the wood-cell and determines adhesive on transverse and, especially, shear properties of the cell wall material.

3.4. Wood cell morphology

In every plant water is the constituent for proper growth. Naturally environment has developed mechanism to absorb, translocate, store and utilize water. In wood cell there are vast network of conduits which made from “xylem and phloem fillers extended throughout the plant” (Merhaut,1999) . These tissues working like human circulatory blood system are continuing from tree roots till every

leaf. In water transport system phloem tissues which are made from living elongated connected cells responsible for nutrients and sugars transferring. Process is produced by the leaves to the metabolically active areas. Xylem also has elongated cells structure. Once cell dies it still remains in process and acts as pipeline to transport water all over the tree. Xylem tissue is one of the main elements in wood cell microstructure system.

Main principal in new layers development is water transpiration. When water evaporates through specialized openings in the leaves, called stomates (Faulkner, 1999), evaporation creates a negative vapor pressure which pulls water from xylem that was transferred from the leaf. Formed tension will be extended through the rest xylem column. But water within the wood is not under positive pressure, than if you cut, or drill you would expect a stream of water to come out. Considering that water transfer process under bark of tree going under negative pressure or suction, water in molecular ratio stands out of both positive and negative electrically charged parts which highly increase particle adhesion. Long chains of water molecules extend all the way from the leaves down to the roots (Vitosh, 1999).

In wood growing cycle xylem are called vessel elements which size vary from 20 to 800 microns (Faulkner, 1999). To connect longitudinally positioned layers vessel walls have very small openings called pits that allow movement of building material (mostly cellulose). For water moving through these elements a continuous column structure is built. Column for water transferring is maintained throughout the tree's life span by two factors. First is capillary action in trees tracheids and secondly is root pressure caused by osmosis from soil into the root tissue. Afterwards it is possible to overcome the hydrostatic form of the water column. (Keillor, 1999)

A wood tracheid is generally showed as a hollow layered structure (Joffre, 2013). "In the wood tissue, the tracheids are surrounded by the middle lamella, which holds the cells together. (Joffre, 2013)" Mainly wood cell consist of parts which core are crystalized or non-crystalized (amorphous). Mathematically it can be described by adding degree of crystallinity to find ratio between "the volume of crystalline cellulose and the total volume of cellulose" (Flores, 2010). Amorphous part may absorb moisture and rapidly change its mechanical properties. Although crystalline part is a polymer build by sugar units softening with increased moisture. The fact that the cell collapses almost immediately after the amorphous cellulose reaches the condition of plasticity, would indicate that yielding in the noncrystalline portion of cellulose would correspond to a mechanism of failure in the wood cell under straining (Flores *et al.*, 2010).

3.5. Wood cell size and topology

In natural cellular materials, such as wood, there are further considerations: the shapes of the cells are clearly influenced by the loads that the material has to carry (Currey, 1984). Mechanical considerations determine the orientation of cells in wood (Dinwoodie, 1981) because of water transferring mechanisms caused by tension in lignin columns. Lignin is the most hydrophobic component in the cell-wall, with relatively stable mechanical properties under moisture changes (Neto *et al.*, 2010).

Before starting ultrasound experiment it is very important to make optical specimen investigation. With nowadays technique is possible to prove Aboav (1970,1980) hypothesis that cell with more sides than average has neighbors which, taken together, have less than average number. This correlation was noted in Smith's (1952, 1964) pictures of soap honeycombs. It concludes that pictures will let to sign angles of wooden cell walls. Particularly woods – have cells so elongated that, in the plane transverse to the direction of elongation, the cell look and behave like a honeycomb (Gibson, Ashby 2001). Photographical investigation, can be provided with CT scanner. The algorithm is created for automatic knot segmentation (Krähenbühl, 2014). Scientists identified it as difficult problem in wet materials, because of same density of knot and plain timber. But with the help of 2D digital contours and state-of-art algorithms he manages to find solution. With his technique is possible to investigate really accurate data. In this topic we are more interested on radial and longitudinal cross-sections. In these directions inside composition of knot could is also observed. The main difference between wood-sells size of knot and plain timber is that macro structure of knot area can be fractured. Important to know from what parts of the wood specimen are taken. It is known that last layers in front of bark are working for water transferring to the leaves. Inner layers of the stem are filled with atmosphere and only keep tension and self-mass. Honeycombs type cell always contains periodic variation in density or cell size as it was noticed in trees growth rings.

3.6. Wood Knots

A wood stem starts to grow radially around a central axis: the pith. This part is the center of the annuals growth rings and the origin of branches. During the growth process, branches grow toward the outside of the trunk. During it growth rings are created and trunk widens covering the branches. Covered branch part is called the knot (Krähenbühl *et al.* 2014) The most significant one are knots with associated grain deviations that mostly affect mechanical parameters of timber beams. To understand what causes knot in plain timber first structure of it should be analyzed. Knot as it depends mostly from its area ratio is distorted grain around plain wood and can behave as incipient crack, when the wood is

loaded. In most cases when wood is under load, failure starts from the knot. Knot area consists of bigger density and perpendicular grain deviation than in plain wood which causes such mechanical differences. There are various types of knots which depends most if the branch inside stem was dead or not. Also, knots can be grouped by whorls. A whorl contains several knots distributed around the pith like the petals of the flower. This phenomenon can be observed only looking from the top of the stem. Also, a knot is the part of a branch that is embedded in the tree stem. When a branch is broken close to the stem, an open wound is formed, making the knot susceptible to attack by fungi and other microorganisms (Pohjamo *et al.*, 2002).

Several methods to capture inhomogeneities like branches in a structural analysis are already known. As a simple option, knots can be considered by means of reduced mechanical material parameters, e.g. the longitudinal elasticity modulus, due to a knottiness factor. Obviously, knottiness can be determined by visual and mechanical methods. By knottiness, strength classes and related material parameters are defined for a structural part made of timber (Jankel, Kaliske 2014).

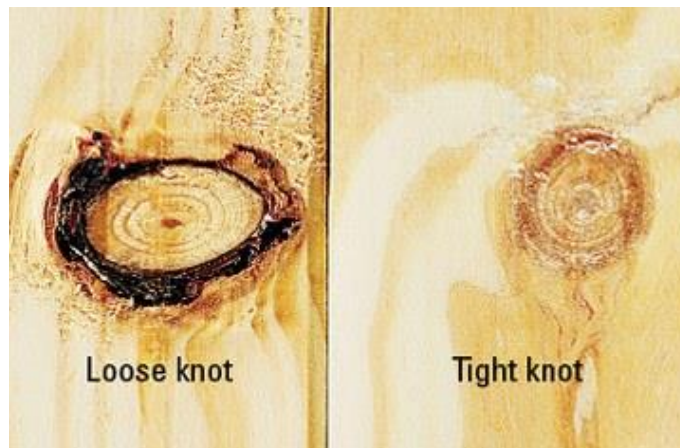


Figure 3.4: Two types of knots encountered in wood grading. Loose knots on the left often fall out as the wood dries. Tight knots such as the one on the right are coalesced with wood but need sealing. (Meredith, 2015)

Through the time algorithms are developed to detect knot area. Sometimes it is interpreted like sub-domain of a 3D tree image. By using photos obtained from X-ray, with CT scanners are possible to use automatic segmentation of tree knots. Due similarity of knot and sapwood densities knot detection is known as a difficult scientific problem. One of the methods is to use a local convexity constraint to guide the knot segmentation inside the wood (Krähenbühl *et al.*, 2014). By iteration step-by-step method area around each knot is segmented independently of the others. This type of detection starts

from the tree pith. With a help of 3D connected component analysis of the knot distance and radius between pith and bark could be extracted (Krähenbühl, 2014).

In some researches to fully understand properties of the knot, its diameter, knot frequency, radial sound-knot (intergrown) length, and radial loose-knot (encased) length should be observed (Moberg, 2001). In this master thesis knot area will be observed with ultrasound device by all possible directions. Need to mention that knot area will have its local coordinate system which will be up to 90° to global coordinate system in longitudinal direction. After first data will be extracted graph of density and elasticity distribution will be made to understand what are differences in knot and plain timber area.

There could be developed three model to characterize knots: model A: knots considered as holes in the specimen; model B; adherent knots, where there is structural continuity of knot material and the rest of the specimen material; and model C: partial contact between knot and beam, artificially simulated by means of a contact spring with a friction value between materials.

For the knot structural understanding first some of the materials and parameters should be considered. As we know the main material set composed of cellulose, hemicellulose and lignin should be the same as in plain timber. Knot as growing in branch, will always be in perpendicular direction to wood grain. For mechanical characteristics knot intersection angle should be known. Without it Young's moduli, Shear moduli and Poisson's ratio should be determined for every wood-cells material. The remaining components represent orthotropic elasticity. The sheet-like stem structures formed by cellulose chains connected by intermolecular hydrogen bonds. These sheets are stacked together by van der Waals forces into a three-dimensional structure, considerably softer in the direction of the hydrogen bonds within the sheets (Hofstetter *et al.*, 2005). In addition, the main mechanism of deformation in the cell-wall is shear, localized in the hemicellulose/lignin matrix, due to the relative displacements among cellulose fibers undergoing rigid body rotation and alignment in the direction of the external loads. Therefore, any increase of the stiffness in the cellulose due to a rise in the degree of crystallinity will not affect significantly the overall mechanical response of the cell-wall under low strain levels since the cellulose fiber will experience predominantly changes in its orientation rather than straining along its own axis (Flores *et al.*, 2010).

4. Elastic Properties

Elastic properties of material describe when material body is deformed and return to its original shape after force is removed. It should imply that deformations produced by low stress below the proportional limit are completely recoverable after load is removed (Cai, Ross, 2006). When the

elastic limit reaches maximum and elastic behavior emerges into plastic behavior material is affected under irreversible deformation. Wood is orthotropic material that shows different elastic behavior in radial, longitudinal and tangential directions. In the experimental part of the master project it will be shown what are the stiffness values in every growing direction and how they differentiate along plain and knotted timber. Still, neither Young's modulus, Shear modulus or Poisson's ratio will be computed in the master project, only the mathematical path will be described in the upcoming sections. All required values for stiffness tensor description will be taken from the reliable and recommended literature sources; Neuhaus 1981, Bodig and Jayne 1982 and Hearmon 1948.

Knowing materials Young's modulus Shear modulus and Poisson's ratios values is possible to calculate stiffness tensor using nine engineering constants that can be found from literature sources or performing mechanical strength experiments in every direction. Data accuracy can be verified providing non-destructive testing.

4.1. Modulus of elasticity

Or Young's modulus, E , is defined as the constant of proportionality between a uniaxial stress σ and resulting axial strain ε , i.e:

$$(4.1) \quad \sigma = E\varepsilon,$$

If a uniaxial tensile stress σ_L will be applied to a cross-section rod of specimen the biaxial state of strain will be obtained, consisting of an axial tensile strain ε_L and a transverse strain ε_T . For most of materials the applied stress and the resulting strains will follow a linear relationship, this is the basis for the definition of the engineering elastic constants.

Elasticity implies that deformations produced by low stress are completely recoverable after loads are removed. The modulus of elasticity (MOE) is one of the variables heavily weighing in material selection and mechanical behavior. MOE plays a key role in decking applications where span between supports meeting specific deflection tolerances (Diaz *et al.*, 2011). When loaded to higher stress levels, plastic deformation or failure occurs. The three moduli of elasticity, which are denoted by E_L , E_R , and E_T , respectively, are the elastic moduli along the longitudinal, radial, and tangential axes of wood. These moduli are usually obtained from compression tests; however, data for E_R and E_T are not extensive. The elastic ratios, as well as the elastic constants themselves, vary within and between species and with moisture content and specific gravity (Green *et al.*, 2002). On the basis of the Haines,

Leban and Herbe (1996) it is possible to assume that it is possible to calculate Young's modulus from the ultrasound measurements using:

$$(4.2) \quad E = \rho v^2,$$

Where ρ is material stiffness and v is calculated velocity of the wood specimen (Haines, Leban, Herbe, 1996). In some examples modulus of elasticity can be observed using some exclusive methods like Taber stiffness tester where for measuring MOE consist of static bending test or dynamic mechanical analysis (DMA) requires only special sample preparation and equipment set up, this method is used in material development studies or for quality control. (Diaz *et al.*, 2011). A Taber stiffness tester bends rectangular specimens to a certain angle with the required bending moment recorded in Taber units also called Taber stiffness. The test presupposes all samples to have the same geometry, thus making the results comparable. In other words, a sample having greater resistance to bending (Klungness, 2000). To give a small introduction to Taber experiment stiffness tester performs a two point (cantilever beam) bending test using a pendulum weighing system. A sample is clamped at the top of the pendulum on the center of rotation and a force is applied to the lower end deflecting the sample to a certain angle (i.e., 7.5° or 15°). The bending moment can be read in Taber units which are equivalent to centimeters. After data is collected from Taber test and modulus of elasticity is acquired. To prove that information corresponds to reality comparison with universal testing machines should be provided. Nether or less, data correlation could cause errors in results. For this master's thesis experiment with Taber stiffness methodology won't be provided.

4.2 Shear modulus

With the wood shear modulus is possible to understand a mentioned material as transverse anisotropic that is observed mostly in the wood because of the much larger longitudinal modulus (E_L) than radial or tangential modulus (E_L or E_R). But, in reality, E_R is typically double E_T (Bodig 1982); this difference should not be ignored for accurate modeling of transverse stresses. In hardwoods, the stiffer radial direction may be due to rays cells (Price 1929; Schniewind 1959). In softwoods, the stiffer radial direction may be due to alignment of cells in radial rows (Price 1929). Whatever the reason, transverse anisotropy causes some unusual experimental results. Bodig (1963; 1965) observed that E_R of Douglas fir increases as specimen thickness increases. In contrast, Hoffmeyer et al. (2000) found that E_R of Norway spruce decreases as gage length increases. Kennedy (1968) measured transverse

modulus as function of loading angle for several species and found that the modulus varies with angle and can even be lower than both E_R and E_T . Shipsha and Berglund (2006) found that E_R of periphery boards far from the pith of Norway spruce is more than double the E_R for boards close to the pith. These observations are a consequence of the transverse anisotropy of wood and of fitting a cylindrical material into a rectangular specimen. They are also influenced by the particularly low transverse shear modulus, G_{RT} , of wood. A low G_{RT} combined with growth ring curvature causes localized deformations that affect modulus experiments (Aicher and Dill-Langer 1996, Aicher et al. 2001; Shipsha and Berglund 2006). Another wood property that may play a role, but is less studied, is the layering of wood into *Earlywood* and *Latewood* material within each growth ring; i.e., the composite structure of solid wood (Nairn, 2006).

The Shear modulus indicates the resistance to deflection of a member caused by shear stresses. The three moduli of rigidity denoted by G_{LR} , G_{LT} , and G_{RT} are the elastic constants in the $L_R L_T$ and R_T planes, respectively. For example, G_{LR} is the modulus of rigidity based on shear strain in the LR plane and shear stresses in the LT and RT planes. Average values of shear moduli for samples of a few species expressed as ratios with E_L are given in various literature (Green *et al.*, 2002).

Consistent with the definition of the Young's modulus, the Shear modulus G , is defined as

$$(4.3) \quad \tau = G\gamma,$$

Where the shear strain is defined in engineering notation, and therefore equals the total change in angle : $\gamma = \theta$. Considering Young modulus calculation provided by Haines, Leban and Herbe (1996) Shear modulus also can be calculated using sound velocity calculated from non-destructive testing.

$$(4.4) \quad G = \rho v^2,$$

Where ρ is material stiffness and v is calculated velocity of the wood specimen. Calculated time have to be measured with transversal transducers. For wood every specimens have to be measured for two times in every growing direction. The crystal theory for solid material is proving if transversal waves is valid: $c_{LR} = c_{RL}; c_{LT} = c_{TL}; c_{TR} = c_{RT}$ (Krautkrämer, 1986). Where first letter of index showing measured direction and second letter showing wood growing direction. Therefore the shear moduli are usually calculated on the basis of the arithmetic mean of the pairwise linked sound

velocities. For example, c_{LT} is the Shear modulus for stress along to longitudinal axis and strain along the tangential axis.

On other side, the variation in values for moduli determination can be explained by normal experimental measurements due to complex ultrasound signals (Baradit, 2012).

4.3 Poisson's Ratio

Poisson's ratios of anisotropic materials could be expressed as functions of normal elastic stiffness, considering the positive definiteness of the stiffness and compliance tensors. Especially for anisotropic materials, where all Poisson's ratios cannot be anymore computed from the Young's and shears moduli and Poisson's ratio strongly depends from materials structure. For isotropic material the Poisson's ratio ν , as the ratio of the transverse strain to the axial strain. For big part of materials the transverse strain is compressive for a tensile applied stress. Poisson's ratio is defined as the negative of this ratio, to give a positive quantity.

$$(4.5) \quad \nu = -\frac{\varepsilon_T}{\varepsilon_L},$$

Poisson's ratio is possible to perform using standard mechanical (tensile) tests or by inversion of the elasticity tensor measured in ultrasonic tests. In order to obtain orthotropic elasticity tensor components in the principal material directions, wave propagation in symmetry planes, more precisely in all principal and three non-principal directions, is necessary.

For wood, the six Poisson's ratios are denoted $\mu_{LR}, \mu_{LT}, \mu_{RL}, \mu_{RT}, \mu_{TL}, \mu_{TR}$. The first subscript refers to the direction of applied stress; the second subscript refers to the direction of the accompanying lateral strain. For example, μ_{LT} is the Poisson's ratio for stress along to longitudinal axis and strain along the tangential axis.

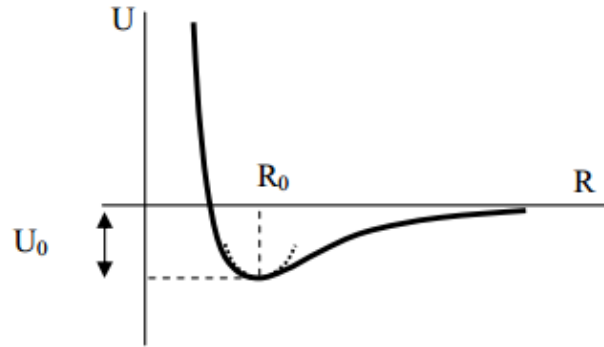
When a member is loaded axially, the deformation perpendicular to the direction of the load is proportional to the deformation parallel to the direction of the load. The ratio of the transverse to axial strain is called Poisson's ratio. The Poisson's ratios are denoted by $\mu_{LR}, \mu_{RL}, \mu_{LT}, \mu_{TL}, \mu_{RT}$, and μ_{TR} . The first letter of the subscript refers to direction of applied stress and the second letter to direction of lateral deformation. More precisely, normal stiffnesses are related to purely longitudinal phase velocities, and shear stiffnesses are related to purely transversal phase velocities For example, μ_{LR} is the Poisson's ratio for deformation along the radial axis caused by stress along the longitudinal axis. Values for μ_{RL} and μ_{TL} are less precisely determined than are those for the other Poisson's ratios.

Poisson's ratios vary within and between species and are affected by moisture content and specific gravity (Green *et al.*,2002).

Poisson's ratio is the negative ratio of a lateral to an applied strain. As a result, it is independent of relative density; it depends only on the cell geometry. Dimensional arguments of the type used to calculate the Young's modulus and the shear modulus offer no insight into its dependence on cell geometry (Gibson, Ashby 2001).

5. Mathematical Description of Stiffness Derivation for Orthotropic Materials

Elastic properties of solid are determined by interatomic forces acting on atoms when they are displaced from equilibrium positions. At small deformations these forces are proportional to the displacements of atoms. As an example, consider a 1D solid. A typical binding curve has a minimum at the equilibrium interatomic distance R_0 :



Differentiating Eq. (1), $F = -\frac{\partial U}{\partial R}$, we obtain force F acting on the atom:

$$(5.1) \quad F = -ku,$$

The constant k is an interatomic force constant. Eq.(5.1) represents the simplest expression for the *Hooke's law* showing that the force acting on an atom, F , is proportional to the displacements u . This law is valid only for small displacements and characterizes a *linear region* in which the restoring force is linear with respect to the displacements of atoms.

The elastic properties are described by considering a structure as a homogenous continuum medium rather than a periodic array of atoms. In 1D case, $F = -ku$, where u is a change in the wood cell length under applied force F .

$$(5.2) \quad \sigma = \frac{F}{A} = \left(\frac{-kL}{A}\right) \left(\frac{u}{L}\right) = C\varepsilon,$$

Where A is the area of cross section, and L is the equilibrium length of the 1D structure. The stress σ is defined as the force per unit area and the strain ε is the dimensionless constants which describe the relative displacement (deformation).

For wood, elastic properties can be defined by the generalized Hooke's law relating the average volume of stress $[\sigma_{ij}]$ to the average volume of the strains $[\varepsilon_{kl}]$ by the elastic constants $[C_{ijkl}]$ in the form:

$$(5.3) \quad [\sigma_{ij}] = [C_{ijkl}] \cdot [\varepsilon_{kl}],$$

Or

$$(5.4) \quad [\varepsilon_{kl}] = [S_{ijkl}] \cdot [\sigma_{ij}],$$

Where $[C_{ijkl}]$ are termed elastic stiffnesses and $[S_{ijkl}]$ the elastic compliances, and i,j,k , or l correspond to 1,2,3, or 4. Stiffnesses and compliances are fourth-rank tensors.

In a general cases are formulated as follows:

- (i) Forces are applied in terms of *stress* σ , and determine displacements of atoms which are described in terms of *strain* ε .
- (ii) Elastic constants are defined C relating σ and strain ε , so that $\sigma = C \varepsilon$.
- (iii) $[C_{ijkl}]$ could be written, following the general convention on matrix notation, as $[C_{ij}]$, in terms of two-suffix stiffnesses. Similarly, $[S_{ijkl}]$ could be written as $[S_{ij}]$ or $[S]$.

It is much simple to write given equations in the following form:

$$(5.5) \quad [\sigma] = [C] \cdot [\varepsilon]$$

And

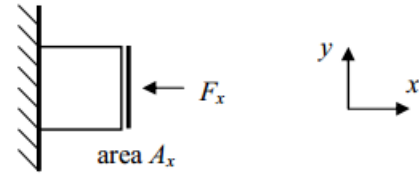
$$(5.6) \quad [\varepsilon] = [S] \cdot [\sigma]$$

It is apparent that the stiffness matrix $[C]$ is the inverse of the compliance matrix $[S]$, as $[C] = [S]^{-1}$ and $[S] = [C]^{-1}$. Experimentally, the terms of the $[C_{ij}]$ matrix could be determined from ultrasonic measurements, where those of the $[S_{ij}]$ could be determined from static test. In this master thesis only ultrasonic measurements will be provided, and the stiffness matrix $[C]$ for anisotropic material will be formulated only using trusted literature sources.

Stress has a meaning of local applied “pressure”. It has $\sigma_{ij} = \sigma_{ij}(\mathbf{r})$.

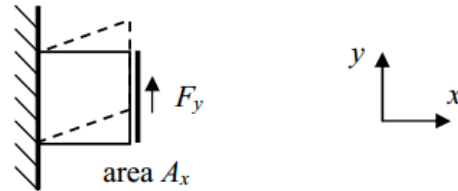
Compression stress (σ_{xx} σ_{yy} σ_{zz}):

$$(5.7) \quad \sigma_{xx} = \frac{F_x}{A_x}$$

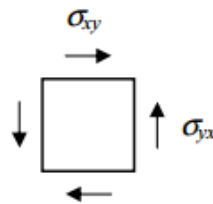


Shear stress (σ_{xy} σ_{yz} σ_{xz} σ_{zx} σ_{yx} σ_{zy}):

$$(5.8) \quad \sigma_{yz} = \frac{F_y}{A_x}$$



Shear forces must come in pairs in converse angular acceleration inside the crystal:



That makes the stress tensor diagonal, i.e.

$$(5.9) \quad \sigma_{ij} = \sigma_{ji},$$

Strain determines relative atomic displacement:

$$(5.10) \quad \varepsilon_{ij}(\mathbf{r}) = \frac{du_i}{dx_j},$$

Where u_i is displacement in “ i ” direction and x_j is the direction along which u_i may vary.

Compression strain (σ_{xx} σ_{yy} σ_{zz}):

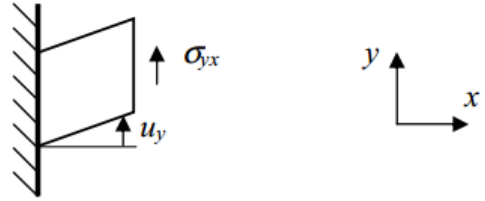
$$(5.11) \quad \varepsilon_{ij} = \frac{du_x}{dx},$$

In a homogenous crystal ε_{xx} is a constant $\varepsilon_{xx} = \frac{u}{L}$, where u is the change in the crystal L .

Shear strain (ε_{xy} ε_{yz} ε_{xz} ε_{zx} ε_{yx} ε_{zy}):

(5.12)

$$\varepsilon_{ij} = \frac{du_j}{dx}$$



Since σ_{ij} and σ_{ji} must always be applied together, we can define shear strains symmetrically:

(5.13)

$$\varepsilon_{ij} = \varepsilon_{ji} = \frac{1}{2} \left(\frac{du_i}{dx_j} + \frac{du_j}{dx_i} \right).$$

5.1. Elastic symmetry

The simplest elastic symmetry is that of an isotropic solid, with only two independent constants, λ and μ . The relationships between those constants are shown as follows:

(5.14)

$$\mu = \frac{E}{2(1+\nu)},$$

(5.15)

$$\lambda = \frac{E \cdot \nu}{(1+\nu) \cdot (1-2\nu)},$$

(5.16)

$$K = \frac{E}{3(1-2\nu)} = \lambda + \frac{2}{3}\mu,$$

Where E is Young's modulus (which is the ratio of longitudinal stress to longitudinal strain in the same direction of a rod), μ is the shear modulus (which is the ratio of the deviatoric stress to the deviatoric strain), ν is the Poisson's ratio (the ratio of the transverse contraction of a samples to its longitudinal extension, under tensile stress), and K is the bulk modulus, with λ and μ the Lamé coefficients.

The velocity of propagation of a bulk longitudinal wave in an infinite isotropic solid, initially assumed to be stress-free, is related to the elastic constants as:

(5.17)

$$V_L = \sqrt{\frac{E_{11}}{\rho}} = \sqrt{\frac{\lambda + 2\mu}{\rho}},$$

Where ρ is the density, and λ and μ are the two Lamé constants.

The velocity of propagation of the transverse wave is related to the elastic constants by:

$$(5.18) \quad V_T = \sqrt{\frac{\mu}{\rho}},$$

Elastic constants C relate the strain and the stress in a linear fashion:

$$(5.19) \quad \sigma_{ij} = \sum_{kl} C_{ijkl} \varepsilon_{kl},$$

Eq. 5.19 is a general form of the Hooke's law. The matrix C in a most general form has 81 components. However, due to the symmetrical form of σ_{ij} and ε_{ij} – each of the have 6 independent components, we need only 36 elastic constants by C_{mn} , where indices m and n are defined as 1= xx , 2= yy , 3= zz for the components. For example, $C_{11} = C_{xxxx}$, $C_{12} = C_{xyxy}$, $C_{44} = C_{yzyz}$.

Therefore, the general form of the Hooke's law is given by

$$(5.20) \quad \begin{bmatrix} C_{11} & C_{12} & C_{13} & 0 & 0 & 0 \\ C_{21} & C_{22} & C_{23} & 0 & 0 & 0 \\ C_{31} & C_{32} & C_{33} & 0 & 0 & 0 \\ 0 & 0 & 0 & C_{44} & 0 & 0 \\ 0 & 0 & 0 & 0 & C_{55} & 0 \\ 0 & 0 & 0 & 0 & 0 & C_{66} \end{bmatrix}$$

The following is a brief discussion of the relationships between the engineering elastic parameters and the terms of stiffness and compliance matrices for solid wood, considered as an orthotropic material, and for composites of wood based materials (plywood, flakeboards, fiberboards, etc.) expected to exhibit transverse isotropy. (Love 1944; Hearmon 1961; Green and Zerna 1968; Jayne 1972; Bodig and Jayne 1982; Guitard 1987).

First we have to consider the orthotropic symmetry of solid wood. The terms of the compliance matrix are given in Eq. (5,21):

$$(5.21) \quad \begin{bmatrix} S_{11} & S_{12} & S_{13} & 0 & 0 & 0 \\ S_{21} & S_{22} & S_{23} & 0 & 0 & 0 \\ S_{31} & S_{32} & S_{33} & 0 & 0 & 0 \\ 0 & 0 & 0 & S_{44} & 0 & 0 \\ 0 & 0 & 0 & 0 & S_{55} & 0 \\ 0 & 0 & 0 & 0 & 0 & S_{66} \end{bmatrix}$$

The physical significance of the compliances is as follows:

- $S_{11} S_{22} S_{33}$ relate an extensional stress to an extensional strain, both in the same direction. For the particular symmetry of solid wood this relation gives the Young's moduli E_L, E_R, E_T .
- $S_{12} S_{13} S_{23}$ relate an extensional strain to a perpendicular extensional stress. In this way the six Poisson's ratios can be calculated.
- $S_{44} S_{55} S_{66}$ relate a shear strain to a shear stress in the same plane, and are inverse of the terms $C_{44} C_{55} C_{66}$, corresponding to planes 23, 13, and 12.

The relationships between the stiffness terms and the compliance terms (Bodig and Jayne 1982) for the orthotropic solid are:

$$(5.22) \quad \begin{aligned} C_{11} &= \frac{S_{22} \cdot S_{33} - (S_{23})^2}{S} \\ C_{22} &= \frac{S_{11} \cdot S_{33} - (S_{13})^2}{S} \\ C_{33} &= \frac{S_{22} \cdot S_{33} - (S_{12})^2}{S} \\ C_{12} &= \frac{S_{21} \cdot S_{33} - S_{23} \cdot S_{31}}{S} \\ C_{13} &= \frac{S_{31} \cdot S_{22} - S_{21} \cdot S_{32}}{S} \\ C_{23} &= \frac{S_{31} \cdot S_{12} - S_{11} \cdot S_{32}}{S} \end{aligned}$$

Where

$$S = S_{11} \cdot S_{22} \cdot S_{33} + 2S_{12} \cdot S_{23} \cdot S_{31} - S_{11} \cdot S_{23}^2 - S_{22} \cdot S_{13}^2 - S_{33} \cdot S_{12}^2$$

The terms of the compliance matrix are similarly related to the terms of the stiffness matrix, with the terms S replaced by the terms C .

When the axes are labeled 1,2,3 engineering constants are related to the compliances in the following way:

$$(5.23) \quad \begin{bmatrix} \frac{1}{E_1} & -\frac{\nu_{12}}{E_2} & -\frac{\nu_{13}}{E_3} & 0 & 0 & 0 \\ -\frac{\nu_{21}}{E_1} & \frac{1}{E_2} & -\frac{\nu_{23}}{E_3} & 0 & 0 & 0 \\ -\frac{\nu_{31}}{E_1} & -\frac{\nu_{32}}{E_2} & \frac{1}{E_3} & 0 & 0 & 0 \\ 0 & 0 & 0 & \frac{1}{G_{23}} & 0 & 0 \\ 0 & 0 & 0 & 0 & \frac{1}{G_{13}} & 0 \\ 0 & 0 & 0 & 0 & 0 & \frac{1}{G_{12}} \end{bmatrix} = [S]$$

Finally, it is worth recalling the relationships between the terms of stiffness matrix and the technical constants:

$$(5.24) \quad \begin{aligned} C_{11} &= (1 - \nu_{23} \cdot \nu) \cdot [E_2 \cdot E_3 \cdot S]^{-1} \\ C_{22} &= (1 - \nu \cdot \nu_{13}) \cdot [E_1 \cdot E_3 \cdot S]^{-1} \\ C_{33} &= (1 - \nu \cdot \nu_{12}) \cdot [E_1 \cdot E_2 \cdot S]^{-1} \\ C_{12} &= (\nu_{21} + \nu_{23} \cdot \nu_{31}) \cdot [E_2 \cdot E_3 \cdot S]^{-1} \\ C_{13} &= (\nu_{13} + \nu_{12} \cdot \nu_{23}) \cdot [E_2 \cdot E_1 \cdot S]^{-1} \\ C_{23} &= (\nu_{32} + \nu_{31} \cdot \nu_{12}) \cdot [E_1 \cdot E_3 \cdot S]^{-1} \\ C_{44} &= G_{23}; C_{55} = G_{13}; C_{66} = G_{12}; \end{aligned}$$

And

$$(5.25) \quad S = [1 - \nu_{12} \cdot \nu_{21} - \nu_{23} \cdot \nu_{32} - \nu_{13} \cdot \nu_{31} - 2\nu_{21} \cdot \nu_{32} \cdot \nu_{31}] \cdot (E_2 \cdot E_2 \cdot E_3)^{-1}$$

For an isotropic solid, the relationships (Green and Zerna 1968) between the Poisson's ratios (defined as the quotient "lateral constriction/longitudinal extension") for a specimen under tension and the elastic constants are:

- For the bulk modulus K

$$(5.26) \quad -1 < \nu < 1/2$$

- For the shear modulus

$$(5.27) \quad G = \frac{E}{2}(1 + \nu)$$

Where ν is the Poisson's ratio, E is the Young's modulus, and G is the shear modulus, also called the Coulomb modulus.

The strain energy function is positive definite for an homogenous isotropic elastic continuum. This means that $K > 0$ and $G > 0$. Consequently $E > 0$ and $(1 - 2\nu) > 0$ or $(1 - \nu) > 0$. The boundary conditions for Poisson's ratios are:

$$(5.28) \quad -1 < \nu < 1/2$$

For an orthotropic solid, the question is more complex due to the six Poisson's ratios, corresponding to the three symmetry planes. Bearing in mind that the strain energy function W must be defined as positive, we form:

$$(5.29) \quad W = \frac{1}{2} \cdot C_{ijkl} \cdot \varepsilon_{ij} \cdot \varepsilon_{kl} > 0$$

And similarly

$$(5.30) \quad W = \frac{1}{2} \cdot S_{ijkl} \cdot \sigma_{ij} \cdot \sigma_{kl} > 0$$

Consequently, $C_{ijkl} > 0$ and $S_{ijkl} > 0$, meaning that all the terms of the stiffness and compliance matrices must be positive, or in other words:

$$(5.31) \quad C_{11}, C_{22}, C_{33}, C_{44}, C_{55}, C_{66}, C_{12}, C_{13}, C_{23} > 0$$

$$(5.32) \quad S_{11}, S_{22}, S_{33}, S_{44}, S_{55}, S_{66}, S_{12}, S_{13}, S_{23} > 0$$

For a real material, the Young's modulus and the shear modulus must also be positive definite as:

$$(5.33) \quad E_1, E_2, E_3, G_{12}, G_{13}, G_{23} > 0$$

Considering now the relationships between the terms of the [C] and [S] matrices and the engineering constants, the boundary conditions for all Poisson's ratios of an orthotropic solids can be

concluded. From Equation (5.33) we can establish the simultaneous relationships between all six Poisson's numbers:

$$(5.34) \quad [1 - \nu_{12} \cdot \nu_{21} - \nu_{23} \cdot \nu_{32} - \nu_{13} \cdot \nu_{31} - 2\nu_{21} \cdot \nu_{32} \cdot \nu_{31}] > 0$$

The relationships between two Poisson's ratios, corresponding to a well-defined symmetry plane, are deduced from Eq. (5.31) when terms C_{11} , C_{22} , and C_{33} are considered as

$$(5.35) \quad 1 - \nu_{12} \cdot \nu_{21} > 0; 1 - \nu_{13} \cdot \nu_{31} > 0; 1 - \nu_{32} \cdot \nu_{23} > 0;$$

From these equations we recognize that the corresponding in-plane Poisson's ratios ν_{rq} and ν_{qr} could both have the same sign (+) or (-). On the other hand, the relationship between Poisson's ratios and Young's moduli is $-\frac{\nu_{rq}}{E_r} = -\frac{\nu_{qr}}{E_q}$ and

$$(5.36) \quad \nu_{rq} = \nu_{qr} \cdot E_q/E_r$$

However, for anisotropic solids it is possible to have $E_r > E_q$ and therefore $\nu_{qr} > 1$.

Indeed, negative values of Poisson's ratios or values greater than 1 may contradict our intuition if our main experience is dealing with isotropic solids, but such data have been reported for composite materials (Jones 1975) and for foam materials (Lipsett and Beltzer 1988), cellular materials (Gibson and Ashby 1988), crystals, wood (McIntyre and Woodhouse 1986), and wood-based composites (Bucur and Kazemi-Najafi 2002).

Referring to the analysis above, the assumption of orthotropy suggests that nine independent stiffnesses or compliances characterize the elastic behavior of solid wood analyzed in a rectangular coordinate system. As a consequence, we find 12 engineering parameters: three Young's moduli, three shear moduli, and six Poisson's ratios.

5.2. Elastic Wave Propagation in Anisotropic Media

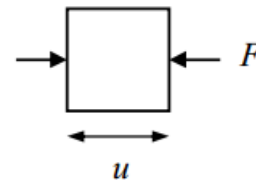
The propagation of waves in isotropic and anisotropic solids has been discussed in many reference books (Angot 1952; Hearmon 1961; Fedorov 1968; Musgrave 1970; Auld 1973; Green 1973; Dieulesaint and Royer 1974; Alippi and Mayer 1987; Rose 1999).

Let us consider first the case of an isotropic solid in which bulk waves are propagating. When the particle motion is along the propagation direction, we have a longitudinal wave. When the particle motion is perpendicular to the propagation direction, we have a shear wave or a transverse wave. In anisotropic materials both longitudinal and transverse waves can propagate either along the principal symmetry directions or out of them. Surface waves can propagate in any direction on any isotropic or anisotropic substrate, and can be used for the characterization of elastically anisotropic solids having piezoelectric properties as well as the characterization of layered solids (Edmonds 1981).

The terms of the compliance matrix are similarly related to the terms of the stiffness matrix, with the terms of stiffness matrix and the technical constants:

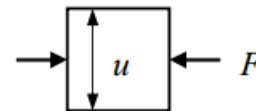
Longitudinal compression (Young's modulus):

$$(5.37) \quad C_{11} = \frac{\sigma_{xx}}{\varepsilon_{xx}} = \frac{F/A}{u/L}$$



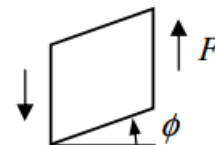
Transverse expansion

$$(5.38) \quad C_{12} = \frac{\sigma_{xx}}{\varepsilon_{xx}}$$



Shear modulus:

$$(5.39) \quad C_{44} = \frac{\sigma_{xx}}{\varepsilon_{xx}} = \frac{F/A}{\phi}$$



5.3. Elastic waves

So far, we have assumed that atoms were at rest at their lattice sites. Atoms, however, are not quite stationary, but can oscillate around their equilibrium positions (e.g., as a result of thermal energy). This leads to lattice vibrations.

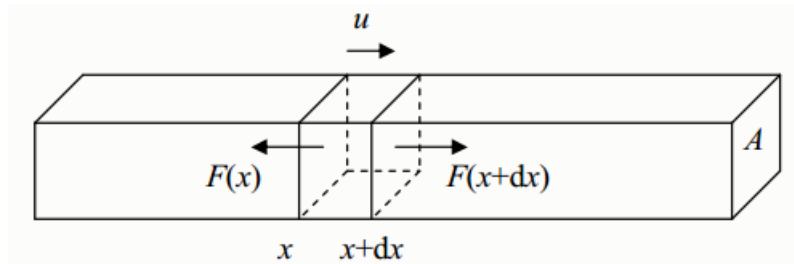
When considering lattice vibrations three major approximations are made:

- (i) It is assumed that displacements of atoms are small, i.e. $u \ll a$, where a is a lattice parameter.
- (ii) Forces acting on atoms are assumed to be *harmonic*, i.e. proportional to the displacements: $F = -Cu$. This is the same approximation which is used to describe a harmonic oscillator.
- (iii) It is assumed that adiabatic approximation is valid – electrons follow atoms, so that the nature of the bond is not affected by vibrations.

The discreteness of the lattice must be taken into account in the example of lattice vibrations. However, when the wavelength is very long, i.e. $\lambda \gg a$, one may disregard the atomic nature and treat the solid as a continuous medium. Such vibrations are referred to as *elastic waves*.

We consider an elastic wave in a long bar of cross-sectional area A and mass density $\rho = M/V$

- (1) First we consider a *longitudinal wave* of compressive/expansion.



We look at a segment of with dx at the point x and denote the elastic displacement by u . According to the Newton's second law

$$(5.40) \quad m \frac{d^2u}{dt^2} = \sum F,$$

That concludes:

$$(5.41) \quad (\rho A dx) \frac{d^2u}{dt^2} = F(x + dx) - F(x),$$

$$(5.42) \quad \rho \frac{d^2u}{dt^2} = \frac{1}{A} \frac{dF}{dx} = \frac{d\sigma_{xx}}{dx},$$

Where we introduced the compression stress σ_{xx} . Assuming that the wave propagates along one of the directions, we can write Hooke's law in the form:

$$(5.43) \quad \sigma_{xx} = C_{11}\varepsilon_{xx},$$

Where C_{11} is Young's modulus. Since $\varepsilon_{xx} = \frac{du}{dx}$, this leads to wave equation

$$(5.44) \quad \frac{d^2u}{dt^2} = \left(\frac{C_{11}}{\rho}\right) \frac{d^2u}{dx^2},$$

A solution if the wave equation has the form of a propagating *longitudinal plane wave*

$$(5.45) \quad \mathbf{u}(x, t) = Ae^{i(qx - \omega t)}\hat{x},$$

Where q is the wave vector,

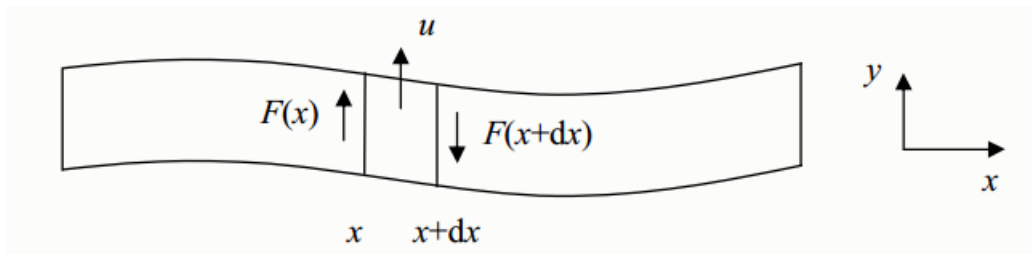
$$(5.46) \quad \omega = V_L q,$$

Is the frequency and

$$(5.46) \quad V_L = \sqrt{\frac{C_{11}}{\rho}}$$

Is the *longitudinal velocity of sound*.

(2) Now we consider a *transverse wave* which is controlled by shear stress and strain.



In this case

$$(5.47) \quad \rho \frac{d^2u}{dt^2} = \frac{d\sigma_{xy}}{dx},$$

Where the shear stress σ_{xy} is determined by the shear modulus C_{44} and shear strain $\varepsilon_{xy} = \frac{du}{dx}$.

$$(5.48) \quad \sigma_{xy} = C_{44}\varepsilon_{xy}.$$

Therefore Eq.(5.48) takes the form

$$(5.49) \quad \rho \frac{d^2u}{dt^2} = C_{44} \frac{d\varepsilon_{xy}}{dx} = C_{44} \frac{d^2u}{dx^2},$$

Resulting the wave equation

$$(5.50) \quad \frac{d^2u}{dt^2} = \left(\frac{C_{44}}{\rho}\right) \frac{d^2u}{dx^2}.$$

This is the equation for the transverse plane wave, which has displacements in the y direction propagates in x direction:

$$(5.51) \quad \mathbf{u}(x, t) = Ae^{i(qx - \omega t)} \hat{\mathbf{y}},$$

Where q is the vector,

$$(5.52) \quad \omega = V_T q,$$

In the frequency, and

$$(5.53) \quad V_T = \sqrt{\frac{C_{44}}{\rho}}$$

Is the *transverse velocity of sound*. Note that there are two linear independent transverse modes characterized by the displacements in modes characterized by the displacements in y and in z directions. For the any of wood direction, by symmetry the velocities if these modes are the same and given by Eq. (5.53).

6. Variety and nature of fundamental sound wave

In the beginning of science of non-destructive evaluation ultrasound wave of propagation was used to propagate through fractured rock masses. Extracted data caused errors by far field explosions or vibrations. After main principles about sound reflection in transversely isotropical materials were known, new theories and mathematical models were created for wood as it is inhomogeneous anisotropic materials. In this chapter types of fundamental sound wave are chosen and described starting from primary and transversal waves that are used in master project to find material's stiffness. In this chapter types of fundamental sound wave will classified describing its propagation in porous materials and basic mathematical formulation will be provided to find main properties.

6.1. Wave propagation in solid and porous materials

Sound can propagate in any kind of medium, not considering its density, porosity or actual phase, creating waves that carry energy. The waves can be understood as moving particles connected with springs disturbed by outer energy making oscillations. The movement of the material is generally confined to small notions, of the material as the wave passes material usually looks just like it did before the wave. Oscillation is considering as single, spherical particles connected with springs. In simplest model particle has only mass (m) and spring has its elasticity coefficient (k). Those two main properties can differentiate or be constant depending from given system. After a source of energy creates the oscillations resulting the wave propagate out from disturbance. If there is finite energy in a confined or short-duration disturbance, the waves will spread out during propagation of bouncing from boundaries and attenuate (become smaller) with distance away from the source or with time after source disappears causing zero disturbance (Braile, 2010).

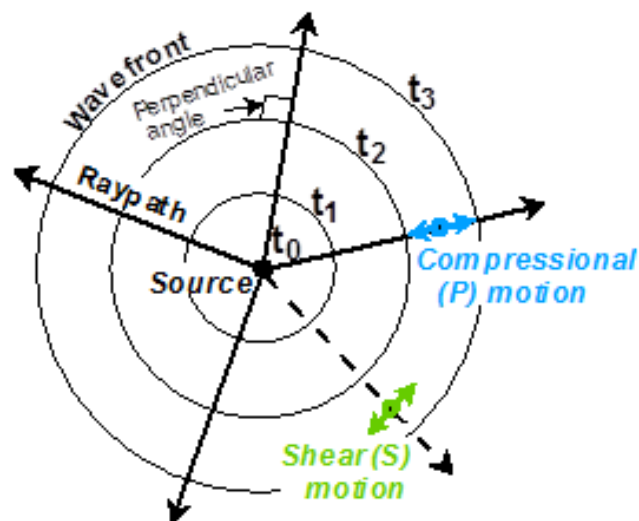


Figure 6.1: Wavefronts and raypaths for the wave propagating from a source.

Three positions (successive times) of the expanding wavefront are shown. Particle motions for P (compressional) and S (shear) waves are also shown. Raypaths are perpendicular to the wavefronts and indicate the direction of propagation of the wave. P waves travel faster than S waves so there will be separate wavefront representations for the P and S waves. If the physical properties of the material through which the waves are propagating are constant, the wavefronts will be circular (or spherical in three-dimensions). If the physical properties vary in the model, the wavefronts will be more complex shapes.

Wood as is multicomponent, hygroscopic, anisotropic, inhomogeneous, discontinuous, inelastic, fibrous, porous, biodegradable, and renewable material (Bodig and Jayne, 1982, p.vii) where structure can be considered as particle grid system connected by springs where ultrasound change is being followed. In this work wood will be studied using non-destructive method with ultrasound that oscillating sound wave pressure with a frequency equal to 100 MHz, that is upper limit of people hearing range. Without nondestructive testing, ultrasound is also used in medicine for ultrasonic imaging or industries for chemical processes acceleration. Fundamentally, waves created by ultrasound source cause particle displacements. Sizes of displacements are so small that it is possible to derive linear relationship between the strains and stresses. Motion of medium, when particles are displaced and accumulated force proportional to the displacement acts on them to restore them to their original position is called elastic wave (Encyclopedia Britannica, 2014).

6.1.1. P-waves

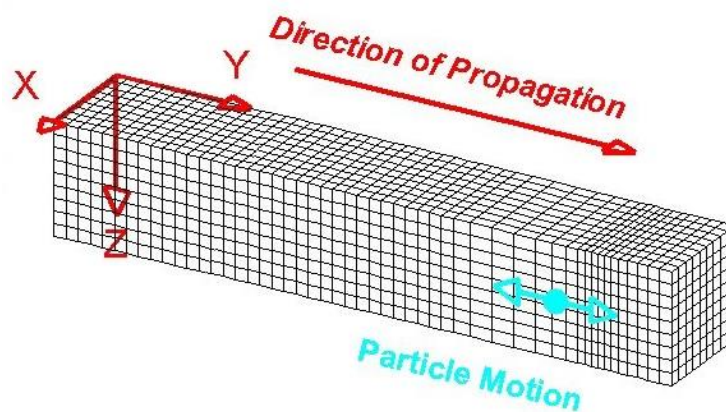


Figure 6.2: Perspective view of elastic P-wave propagation through a grid representing a volume of material

P-waves stand for primary wave with highest velocity and are used in seismology as those travels through medium first. The disturbance that is propagated is a compression followed by a dilatation or extension as it formed from alternating compressions and rarefactions. The particle motion is in the direction of propagation

The material returns to its original shape after the wave has passed. In isotropic material P-wave are always longitudinal making particles in solid material to vibrate along direction of the wave energy.

Cai and Zhao used the method to study P-wave attenuation across linear deformational fractures by considering interfracture wave reflections (Zhao *et al.*, 2006). Their method showed reasonable results of P-wave across linear deformable fractures. It is reasonable to assume that fracture deformation is linear, when the magnitude of the stress waves is insufficient to mobilize nonlinear normal deformation and fictional slip of the fractures (Zhang, 2006). Wave propagation principles are possible to adapt for the theory of composites, where fibers in the form of sheets or material variations are usually used to deliberately make the composite anisotropic along a given direction to induce maximum stiffness (Picotti *et al.*, 2012).

Drawback is limitation in the loss of discreteness of wave attenuation at individual fractures, and the other limitation is the loss of intrinsic frequency dependent property at the fractures. The frequency dependent property is attributed to two mechanisms. First is that the fractures have intrinsic frequency dependent property caused by the displacement discontinuity, and the other mechanism arises by multiple reflections between the fractures. Thus, the stresses across the interface are continuous, but displacements across the interface are discontinuous. Actually, the transmitted wave across parallel fractures can be treated as a wave superposition of transmitted waves arriving at different times, which are caused by the multiple reflections (Zhao, 2006).

Wood structure consists of micro volumes filled with air and could be assigned to aird saturated porous materials. Such examples as polyurethane foam, felt, glass or wood for their small density is used in aerospace, automotive industries or thermal insulation. Wood as one of examples of air saturated porous materials with high density is used only in building constructions.

Because of the heaviness and stiffness compare with sound wave that propagates through material with micro openings or cavities, structural lattice remains steady and without continuous displacements with respect with acoustic excitation. Those materials are characterized with porous rigid structure (Fellah *et all*, 2013).

6.1.2. S-waves

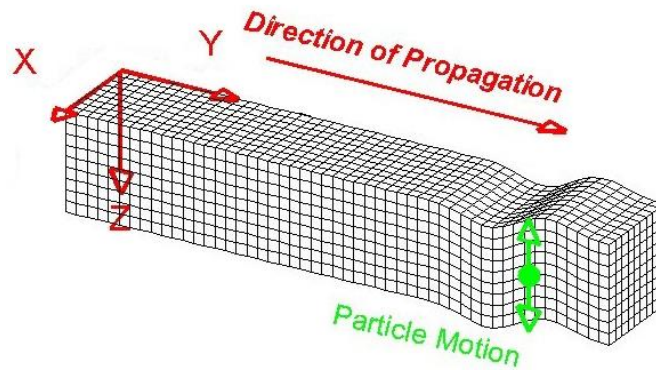


Figure 6.3: Perspective view of elastic S-wave propagation through a grid representing a volume of material

The disturbance that is propagated is an up motion followed by a down motion (the shear motion could also be directed horizontally or any direction that is perpendicular to the direction of propagation). The particle motion is perpendicular to the direction of propagation. The material returns to its original shape after the wave has passed.

S-waves are much slower than P-waves. Waves produced by particle motion are reflected, refracted or scattered slowing the arrival of these waves. Neither or less, several analysis techniques, both in time and frequency domain was considered by S.Crampin (1981) and M.E. Willis, M.N. Toksöz (1983) to determine S-wave velocity in anisotropic and cracked elastic media.

The S-wave is usually decomposed into two components: the SV-wave and the SH-wave that denote to vertical and horizontal, respectively. For anisotropic materials this it's the only way to determine elastic properties. Primary, these techniques were developed for geotechnical applications, but some of them are applicable to wood as well. It was proven that sheets generated by shear-wave are analytically continuous in all anisotropic media, and the sheets must come into contact at least twice as the velocities are unaltered by 180° rotations, because of the symmetry of the tensor transformation (Crampin, 1981). There three types of phases where sheer plates may touch tangentially in convex or concave contact, intersect with each other along the closed curve that is possible only when the closed curve is a circle about the symmetry axis and point singularities, where common points are in cone-shaped projections of the surfaces.

Studies on wave propagation in anisotropic materials aligned with cracks have showed that it is possible to formulate almost any problem and very often solved using considerable numerical solution. Mostly, with shear waves propagation is possible to define cracks in solid materials determining elastic-constants, when cracks are sufficiently small compared with wavelength.

6.1.3. Rayleigh waves

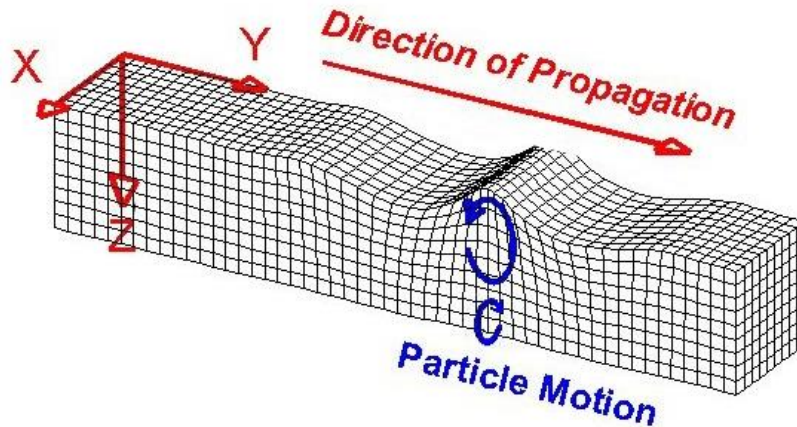


Figure 6.4: Perspective view of Rayleigh-wave propagation through a grid representing a volume of elastic material.

Rayleigh waves are surface waves. The disturbance that is propagated is, in general, an elliptical motion which consists of both vertical (shear; perpendicular to the direction of propagation but in the plane of the raypath) and horizontal (compression; in the direction of propagation) particle motion

The amplitudes of the Rayleigh wave motion decrease with distance away from the surface. The material returns to its original shape after the wave has passed. For Rayleigh wave to propagate a free surface of continuous body have to exist. Important to understand that in a Rayleigh surface wave, particles at the surface trace out a counter-clockwise ellipse, while particle at a depth of more than $1/5^{\text{th}}$ of wavelength trace out clockwise ellipses (Russel, 2013). Rayleigh wave can be seen as the superposition of two separate components: one longitudinal and the other inverse. They propagate along the surface with the same velocity but they have different exponential laws of attenuation with depth. Superposition of different waves gives a null total stress on the boundary of the half space.

In multilayered systems Rayleigh wave is frequency dependent, creating several free vibrational modes which involve different stress and displacement distributions with depth. Looking at material complexity it stands between the stiffness profile and mode of propagation. Multilayered case becomes very complex when wave is propagating away with superposition of the different modes. Still, there is no exact solution to say which mode dominates or to describe the predominance of a mode (Gukunski e Woods 1992). This can be explained physically by the presence of constructive interference between curved ray-paths for continuously varying heterogeneous media and between transmitted and reflected waves for layered media (Achenbach 1984)

Another important note can be made about the path described by particle motion on the ground surface. For the homogeneous half space vertical and horizontal components are 90° out of phase in such a way that as the wave is propagating the particle motion describes a retrograde ellipse. In the case of a layered medium the path is always elliptical but not necessarily retrograde. Moreover in presence of dissipative phenomena (that are likely to occur in soils) the phase difference between vertical and horizontal displacements can be different from 90° and the axes of the ellipse are not necessarily vertical and horizontal respectively (Haskell 1953).

6.1.4. Lamb waves

Lamb waves are used in thin layered materials as they can travel long distances with small attenuation. As lamb waves are transmitted particles oscillate in to different ways. Particles can motion in symmetric that are also called longitudinal mode and anti-symmetrical way are also called flexural mode with respect to the mid surface. Both modes have different phase and group velocities with certain distribution of particle displacement and stress relations along the specimen thickness (Bao, 2003). Propagation characteristics normally are described by the use of dispersion curves based on phase velocity as a function of the emitted product frequency time specimen thickness. A particular lamb wave can be excited if the phase velocity of the incident longitudinal wave is equal to phase velocity for the particular mode. The phase velocity of the incident longitudinal wave is then given by:

$$(6.1) \quad V_p = \frac{V_l}{\sin \varphi},$$

Where V_l the group velocity of the incident longitudinal wave, V_p is the phase velocity of the incident longitudinal wave and φ is the angle of incidence of the incident longitudinal wave.

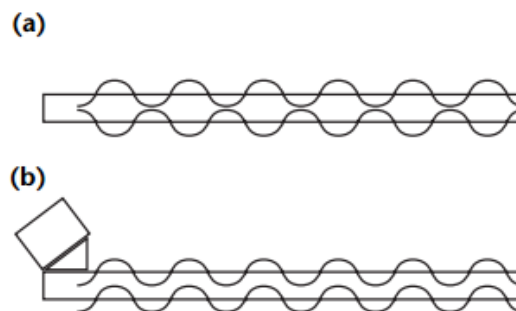


Figure 6.5: Lamb wave propagating in plate: (a) symmetric; (b) antisymmetric

Lamb waves are extremely useful for detection of cracks in thin sheet materials and tubular products. Extensive developments in the applications of lamb waves provides a foundation for the inspection of many industrial products in aerospace, pipe and transportation. The generation of lamb waves can be performed using contact transducers, optical, electromagnetic, magnetostrictive, and air coupled transducers. Because of the complex wood structure using of non-destructive inspection with Lamb waves would be rather inconvenient. Because of specimen geometry and anisometric wood structure non-destructive inspection will be provided using bulk waves with longitudinal and shear waves across all possible grain directions.

6.1.5. Bulk waves

The history of research on wave propagation in anisotropic materials is linked with the development of the theory of elasticity in the early nineteenth century (Love, 1994). Early work by Green in 1839 showed that three wave modes could exist in a general anisotropic medium (Green, 1839). In 1877, Christoffel described the variation in the velocity of wavefronts in anisotropic media with the wavefront normal direction (Christoffel, 1877). He developed mathematical formulae to compute this velocity, referred to as the phase velocity, using plane wave analysis.

In isotropic materials bulk waves propagate with equal velocity in every direction. Wave energy is propagating in two modes: longitudinal and shear. Longitudinal mode is faster because of the vibration of particles is parallel to the propagation of wave energy. Shear mode is slower in wave propagation where particle vibrations are perpendicular to propagation direction. Direction of particles vibration can also be referred as polarization effect.

c_l (longitudinal) and c_s (shear) velocities of the two bulk waves modes can be computed using two elastic properties of the material, as Young's Modulus E and Poisson's ratio ν with material density ρ :

$$(6.2) \quad c_l = \left(\frac{E(1-\nu)}{\rho(1+\nu)(1-2\nu)} \right)^{\frac{1}{2}},$$

$$(6.3) \quad c_s = \left(\frac{E}{2\rho(1+\nu)} \right)^{\frac{1}{2}},$$

Looking into anisotropic case the biggest difference is that elastic waves propagate with a velocity that depends on material's direction. Also, three wave modes can propagate: one longitudinal and two shear waves. However, in anisotropic case propagation modes are referred to as quasi-longitudinal and quasi-shear. For quasi-shear mode is often distinguished whether they are horizontally or vertically polarized. Hence, the wave fronts of quasi-modes do not lie normal to energy propagation direction and do not coincide. It is possible to compute phase and group velocities for anisotropic material using its density and elastic tensor that relates elastic stress and strain. Wood exhibits a lower degree and anisotropy and can be described by fewer independent constants as it will be shown in next section.

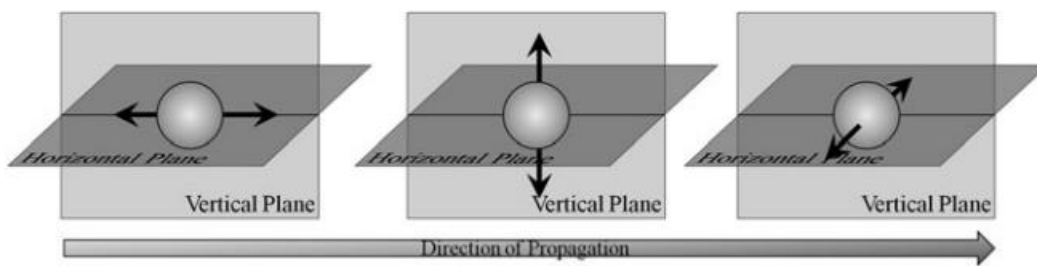


Figure 6.6: Schematic diagram showing (from left to right) pure bulk wave propagation modes with longitudinal, shear-vertical and shear-horizontal polarization.

7. Experimental Part

For wood, to understand its physical properties, a proper method of investigation has to be acquired. For the Master Thesis investigation by non-destructive evaluation system was used. This solution does not require any mechanical interventions or specimen decomposition. Nether or less, understanding of how non-destructive evaluation system works will be described in upcoming chapter. Still, using non-destructive techniques is possible to investigate every material and easily to acquire all stiffness components that are main variables in describing material's physical properties.

7.1. Non-Destructive Testing with Ultrasound Equipment

Experiments in this master project were provided using Non-Destructive testing with ultrasound. Where transmitting transducers were connected with ultrasonic signal preamplifier. Device that is designed to change properties of propagating pulse is sending electrical signal into longitudinal or shear transducers. Technically, both transducers are made in the same manner where piezoelectric crystals are connected with specially set out alternating current to each crystal under backing material. The electrical impulse is changed into mechanical energy that causes micro displacements (vibrations)

under investigated material, only than standing wave is generated that is characterized by high frequencies and sinusoidal oscillations that are infinitely repeated between transducer and receiver, a continuous signal is send to oscilloscope that measures time of propagation.



Figure 7.1: Ultrasonic Signal Preamplifier (5676), Panametrics Inc., Waltham, MA, USA)

Time of propagation under material is the main variable for stiffness calculations excluding material density. Using generalized Hookes law, where elasticity tensor C is a function of the material mass density and the wave propagation velocity (Haines, Leban and Herbe, 1996) is possible calculate stiffness component is any wood growing direction expressed in GPa by using formula:

$$(7.1) \quad C = \rho \cdot v^2 \cdot 10^{-9} [GPa]$$

Where C is calculated material stiffness in GPa, ρ is material density in $[g/mm^3]$ calculated using $\rho = \frac{m}{V}$, where m is mass of specimen given in $[g]$ and V is volume of specimen given by $[mm^3]$ that was calculated using $V = x \cdot y \cdot z$ that is length, width and height of the specimen given by $[mm]$ and v is velocity of sound found by NDET technique in $[mm/\mu s]$.

In this master thesis all 9 engineering values including 3 Young' ratios and 6 Shear modulus were obtained using non-destructive testing with ultrasound. To perform calculations, two types of transducers were used, one for longitudinal (**Figure 7.2**) and second for transverse waves (**Figure 7.3**).



Figure 7.2: Longitudinal Transducers



Figure 7.3: Transversal Transducers

For longitudinal measurements the transducer of 100 kHz was used and stiffness in directions of L_z , L_x and L_y were found. Also, for the shear measurements the transducer of 100 kHz was used and stiffness in the directions of S_{xz} , S_{yz} , S_{yx} , S_{zx} , S_{xy} and S_{zy} were found. The measuring component is hidden under insulating material that in our cases is metal. Main difference between longitudinal and shear transducers is direction of polarization where shear transducers are aligned with the electricity cable connector, this implies that shear transducers emitting transverse waves caused by changed direction of polarization and longitudinal waves that are significantly lower and in wood sometimes are even unnoticeable and can be interpreted as random noise.

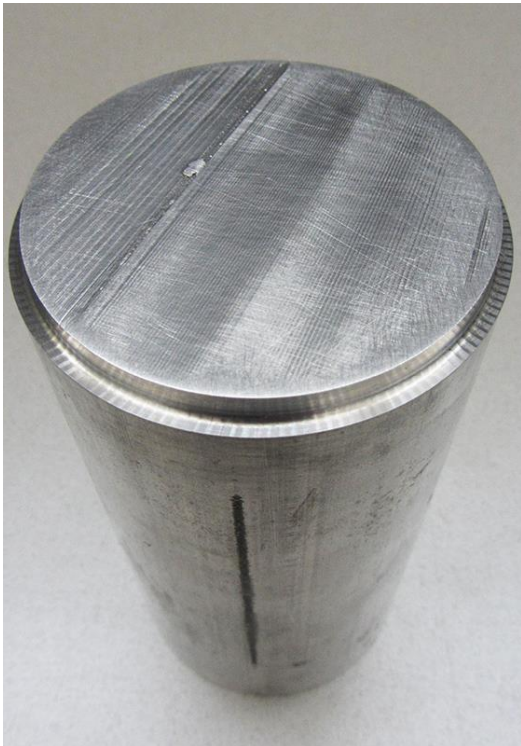


Figure 7.4 Delay line

It was noticed that for transversal wave measurements using 100 kHz with relatively small specimens(average dimensions of specimen is 10x10x20mm) time of propagation error could be higher than obtained values.

For reducing error and getting clear and easy to understand data, the delay line has been used. As a common practice it has been used since the beginning of ultrasonic research when it was beneficiary of radar developments. Radar technology required for delaying electronic signals for microsecond to millisecond durations, that resulted a development of the first ultrasonic delay lines for identifying moving targets (Mason, 1999)

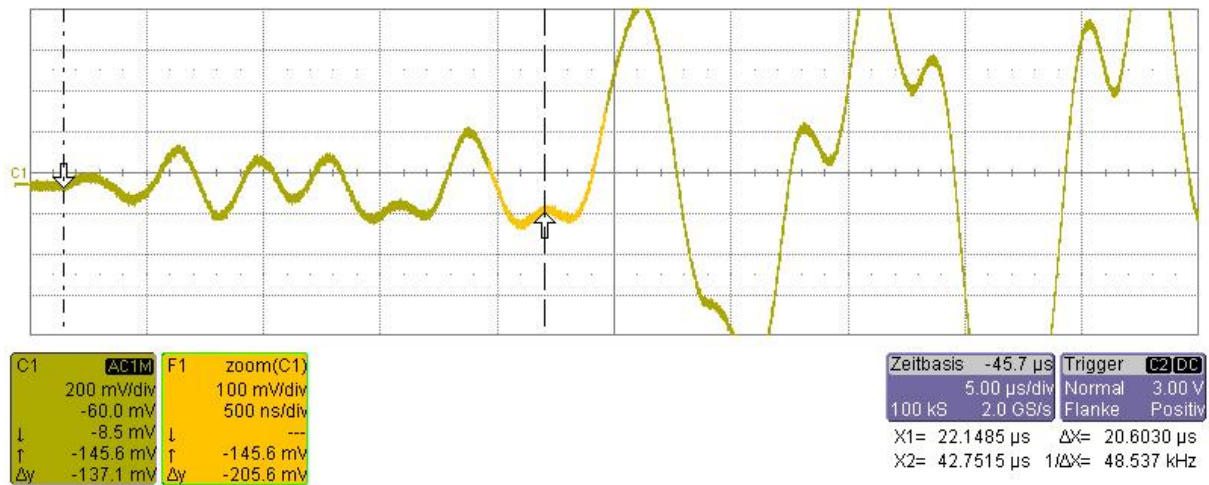


Figure 7.6: Correction time with transversal transducers

Last but not least object used in ultrasound measurement is coupling agent. For both measurements honey was used as a coupling medium. The coupling material is chosen respect to its viscosity. The higher the viscosity the better permeability of sound is approachable. For the correct use in Non-destructive testing with ultrasound, liquid honey is evenly salved throughout transducers surface and covered by plastic film that is used as protection against coupling medium penetration into wood.

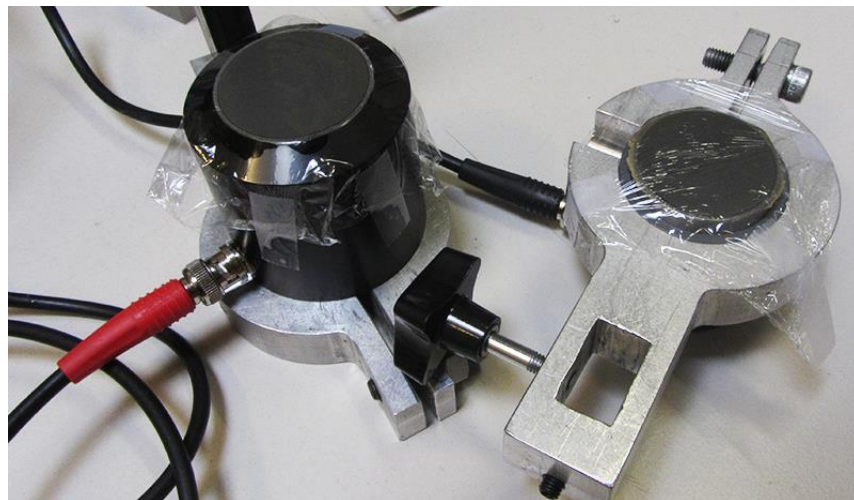


Figure 7.7: Coupling agent (honey) is smeared over entire surface of transducers and covered with plastic film

7.2. Samples

For this master thesis two set of samples were selected to find out wood stiffness characteristics in longitudinal, tangential and radial direction. Both examples were cut into smaller cuboids with desired dimensions of 20mm in height, 10mm in length and 10mm in width. Planned sizes are relatively small and requires precise cutting tools, also cutting it by hand increase

measurement error. Specimens in both examples were cut using thin saw made out of the metal. In the first example samples were cut into the lines and aligned with the step angle of 45° where knot area is in the center of the example. In the second examples wooden plank was divided into 9 rows and 13 columns with the knot in the middle.

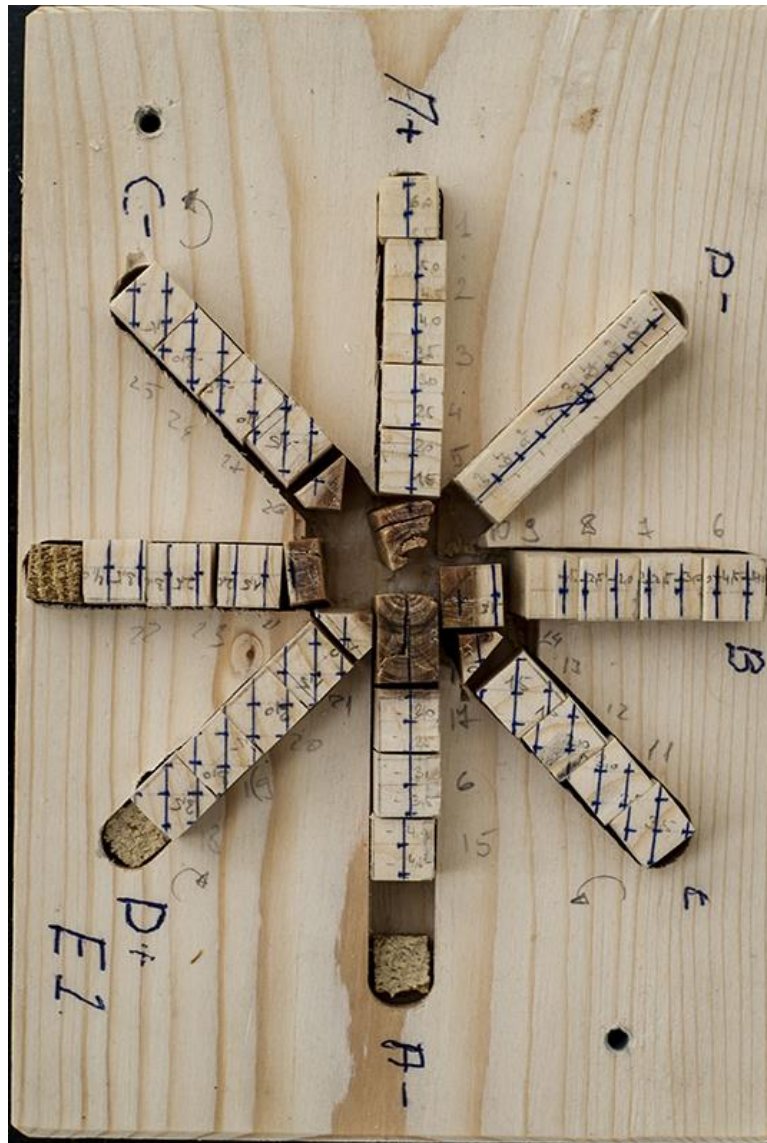


Figure 7.8: Picture of the first sample



Figure 7.9: Picture of the second sample

Both examples were cut from the Norway spruce (*Picea abies*(L.). Totally there were 30 samples (28 in plain timber and 2 in knotted timber) in the first examples and 117 samples (113 in plain timber and 4 in knotted timber) in the second example. All specimens were cut with the same technique, before starting ultrasound measurements they were weighted and measured.

In the master thesis two types of wooden examples will be studied considering its orientation in the wooden plain. One of examples is divided into the grid, where material and cuboid direction of orientation matching with each another and in another example the cuboids are cut from plane with different angles of material direction. In the second examples without stiffness measurements with angle of fiber direction will be measured and will let to answer the question how stiffness is changing approaching knot at certain angle.

7.3. Marking of Specimens

In the first sample specimens were cut and divided into axis with step of 45° where knot is centered in the middle of every axis. Every axis is divided into positive part that indicate specimens set out up to knot and to the negative axis where specimens are set up beneath the knot and beginning of the axis is marked with positive value and begins “A” axis is located in the vertical direction and “B” axis is in horizontal direction. “C” and “D” axis are oblique in 45° between horizontal and vertical axis. “-D” part is left blank because technologically it was not possible to cut specimens from the sample.

For the mark of simplicity, for measurements every specimen was numbered from furthest point approaching knot in clockwise direction and starting from “A” axis. Exact numbering of the knots is shown in **Figure 7.10**.

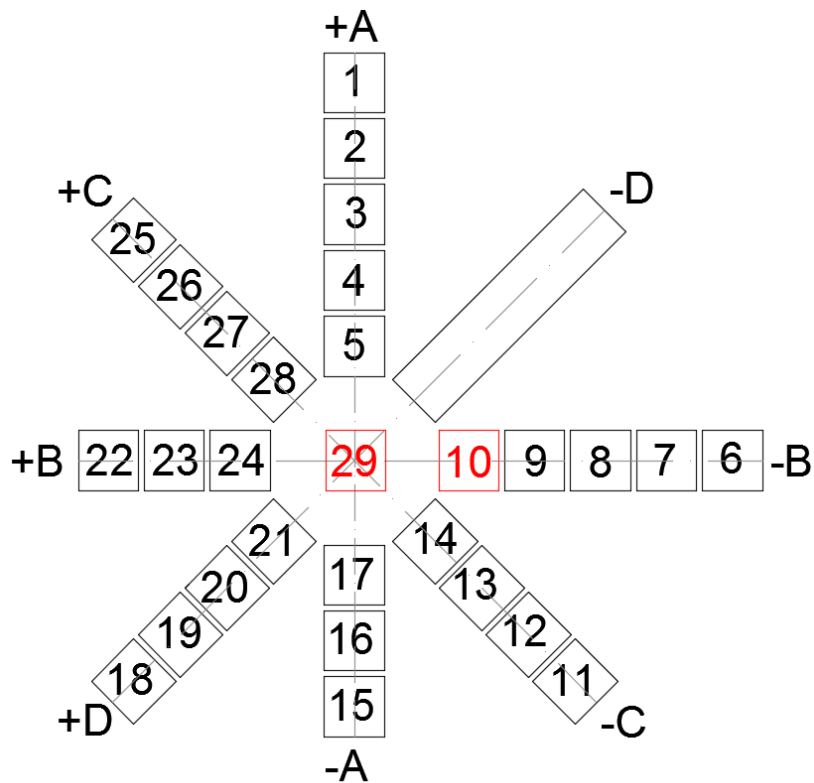


Figure 7.10: First sample specimens marking

I	1	2	3	4	5	6	7	8	9	10	11	12	13
H	1	2	3	4	5	6	7	8	9	10	11	12	13
G	1	2	3	4	5	6	7	8	9	10	11	12	13
F	1	2	3	4	5	6	7	8	9	10	11	12	13
E	1	2	3	4	5	6	7	8	9	10	11	12	13
D	1	2	3	4	5	6	7	8	9	10	11	12	13
C	1	2	3	4	5	6	7	8	9	10	11	12	13
B	1	2	3	4	5	6	7	8	9	10	11	12	13
A	1	2	3	4	5	6	7	8	9	10	11	12	13

Figure 7.11: Second sample specimens marking

For the second sample wooden plank was divided into 9 rows and marked alphabetically starting from A. Every row is divided into 13 equal in size cuboids. Marked specimens in E and F rows are marked as knotted wood and represent middle of the sample, see Figure 7.11. Specimens marked in red color represent knotted wood and require additional explanation that will follow in the next chapter

7.4. Measuring of specimens

Before starting ultrasound experiments specimens are measured and weighted. In master project two type of wood is investigated, plain and knotted timber. In will be examined what are the main differences between those two type of wood from aspects of physical and elastic properties. Every specimen was measured using caliper with $\pm 0,02$ mm error in two places for every side deriving an average length. It was assumed that required dimensions for every specimen should be 20 mm in height, 10 mm in length and 10 mm in width, the average values of specimen size for every sample are:

Table 7.1: First sample average dimensions of specimen

First sample (mm) 28 specimens		Standard deviation	Standard error
Length (x)	10,14	0,40	0,08
Width (y)	9,95	0,23	0,04

Height (z)	20,20	0,03	0,01
------------	-------	------	------

Table 7.2: Second sample average dimensions of specimen

Second sample (mm) 117 specimens		Standard deviation (mm)	Standard error (mm)
Length (x)	10,05	0,11	0,02
Width (y)	10,01	0,27	0,01
Height (z)	20,03	0,06	0,01

Provided values in above shown tables proves that samples were cut with minimal errors in qualitatively condition and it will be possible to provide non-destructive test with ultrasound on them from the set values that was fixed before starting the experiment.

All specimens were weighted using scales with 0,01 error. Here the average values are given with average mass, volume and density of the specimen.

Table 7.3: Average physical properties of the first and second sample

	<i>Mass (g)</i>	<i>Volume (mm³)</i>	<i>Density (mm³/g)</i>
First (27 specimens)	1,08	2039,27	528,20
Standard deviation	0,11	85,56	43,68
Standard error	0,02	16,17	8,25
Second (117 specimens)	1,02	2014,96	508,03
Standard deviation	0,11	58,56	47,62
Standard error	0,01	5,41	4,41

Notice that in the first sample values of 10 and 29 specimen were not included into calculations of average volume and density of the specimen. Mentioned specimen consists partly in 10 and fully in 29 from knotted wood and will be examined separately from all specimens. Notice that in the second sample all specimens were used to calculate and show average value of specimen mass, volume and density.

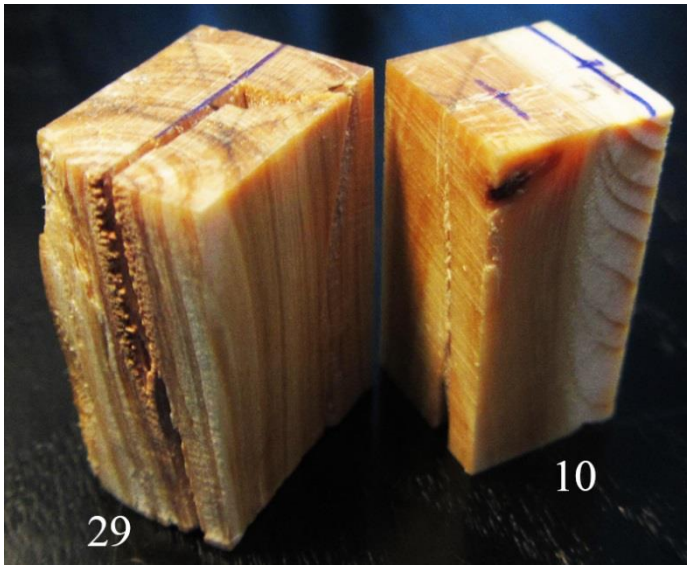


Table 7.4: Specimen 10 and 29 physical characteristics

Number	10	29
Length_X (mm)	9,78	10,05
Width_Y (mm)	10,03	14,55
Height_Z (mm)	20,25	20,23
Mass	1,88	2,94
Volume	1984,39	2957,45
Density	947,40	994,10

Figure 7.12: 10 and 29 specimen from the first sample

From “10” specimen it was noticed that half of specimen consist from plain timber and half of it made from knotted timber. In this specimen is very easy to notice threshold between knotted and plain timber where angle of fiber is changed up to 90°. Same is in “29” specimen that consist only from knotted material that is characterized by slightly darker color and almost twice higher than average density. For stiffness distributions, all specimens from **Figure 7.12** were included into stiffness around of the axis calculations. Specimen 29 was measured with ultrasound twice along vertical (A) and horizontal (B) axis.

From second sample specimens E6; E7; F6 and F7 were marked and selected for more precise verification. As it was observed from the first sample, specimens in knot are having at least twice higher density than average. The fact that knotted wood is characterized twice as higher density as average density of plain timber will let us understand if this physical property somehow changes measurements of stiffness.

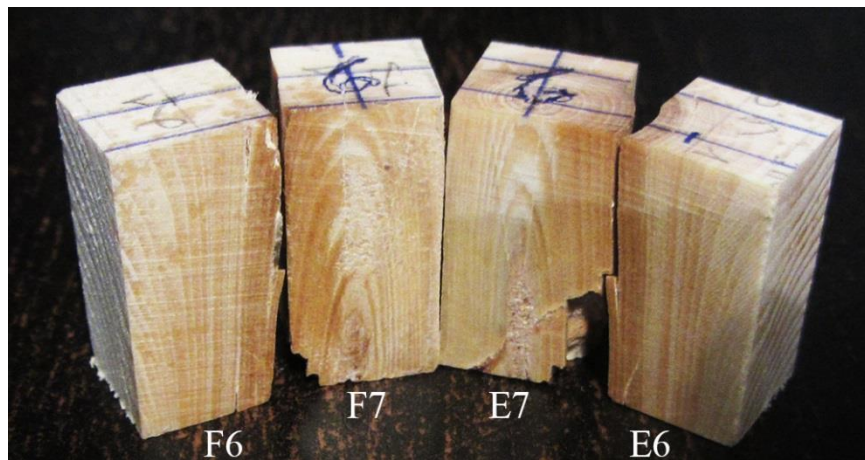


Figure 7.13: Knotted specimens from second example

Table 7.5:Physical characteristics of second example knot

Number	Length_X(mm)	Width_Y(mm)	Height_Z(mm)	Mass(g)	Volume(mm ³)	Density
E6	10,11	10,20	20,14	0,86	2076,88	813,72
E7	10,05	10,28	20,20	1,02	2075,55	958,78
F6	10,60	10,08	20,1	1,63	2146,58	773,82
F7	10,20	10,10	20,2	1,69	2081,00	812,72

7.5. Results

After physical properties are recorded, time of sound wave propagation in the material is founded. Using generalized Hooke's law stiffness of longitudinal and shear component of every material's direction are calculated. Results of stiffness distribution are presented in graphs. For the first sample graphs are showing stiffness distribution along the axis including stiffness properties calculated from inside and around knot area. Graph from D axis is half shorter as for technological reasons it was not possible to obtain specimens from “-D” part. For the second sample plots are representing stiffness distribution for every component in every element.

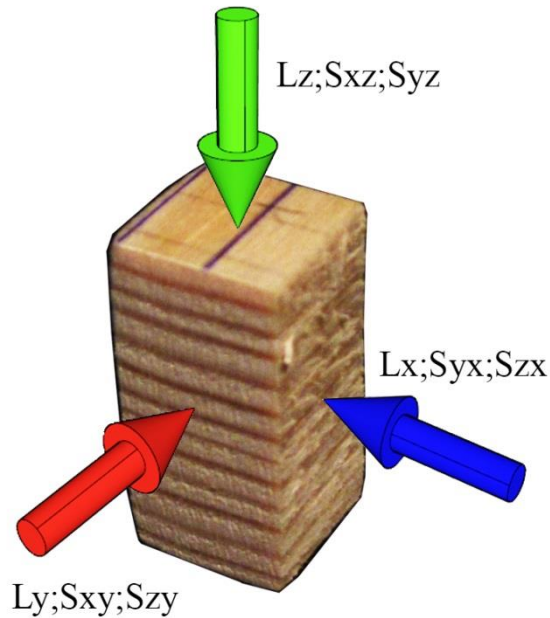


Figure 7.14: Schematical representation of geometrical coordinate system of single specimen, where blue is **X** axis with length of 10 mm, red is **Y** axis with length of 10 mm and green is **Z** axis with height of 20mm.

Experiments are done using non-destructive evaluation technology where standing wave is formed between the receiver and transducer, where honey under polyethylene film is used as the coupler. For longitudinal and shear measurements different transducers of 100 kHz frequency were used. Signal is sent from pulse/receiver converter where it is possible to set pulse repetition frequency, pulse voltage, transducer frequency and gain (dB). All results that include graphs of standing wave where times of propagating wave can be marked are shown in Oscilloscope.

Wood is anisotropic material with three different directions. To calculate stiffness for one direction longitudinal and two shear waves times have to be found. For every specimen, 9 measurements are taken with one longitudinal and two shear wave times along every direction. For longitudinal wave propagation time, transducer of 100 kHz is used that is designed to emit only longitudinal waves. 100 kHz longitudinal and shear transducers are used because of the small specimen size where wavelength of sound propagation has to be higher than width of the specimen.

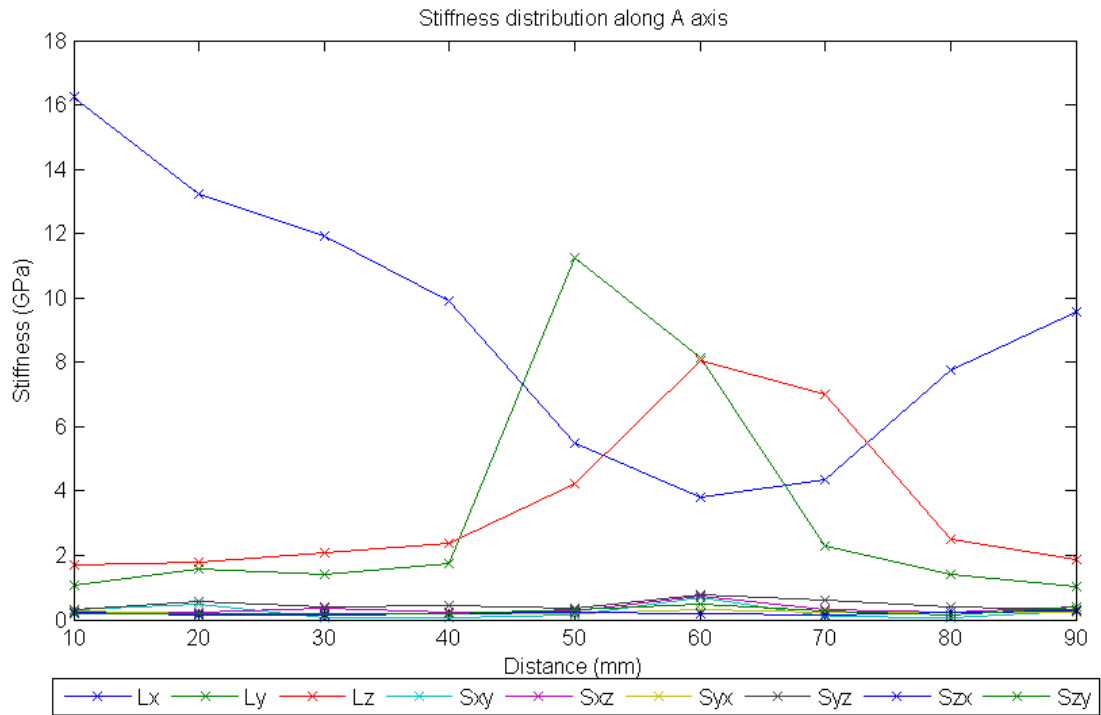


Figure 7.15: Stiffness distribution along A axis

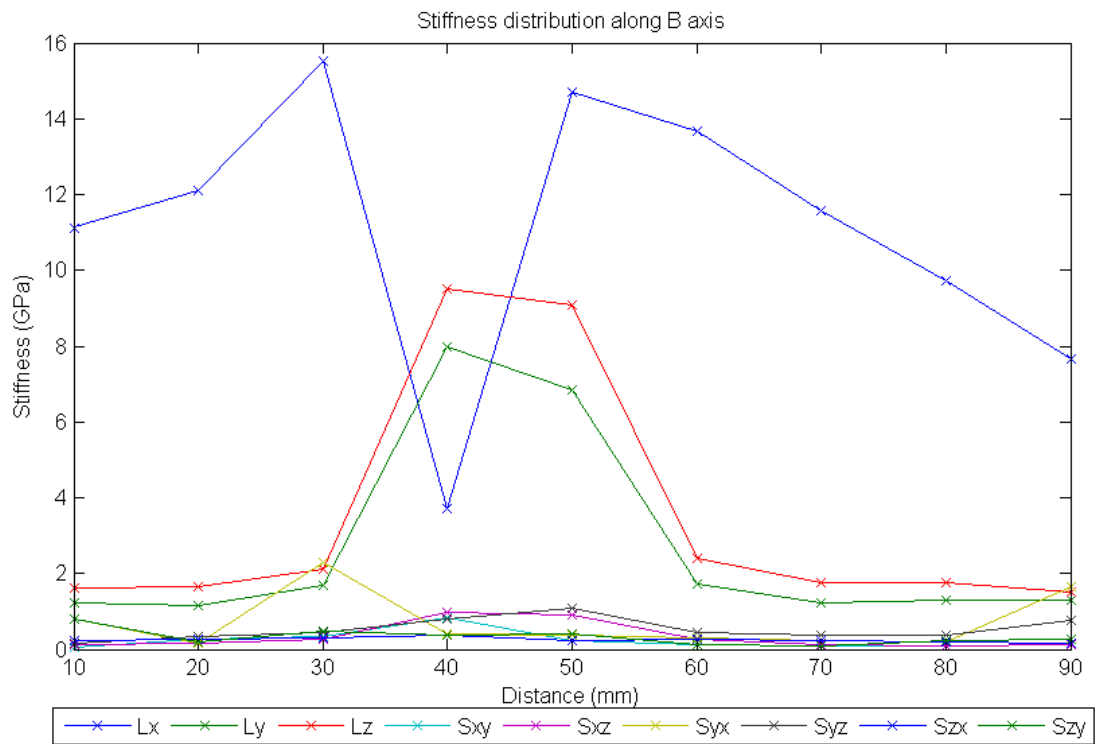


Figure 7.16: Stiffness distribution along B axis

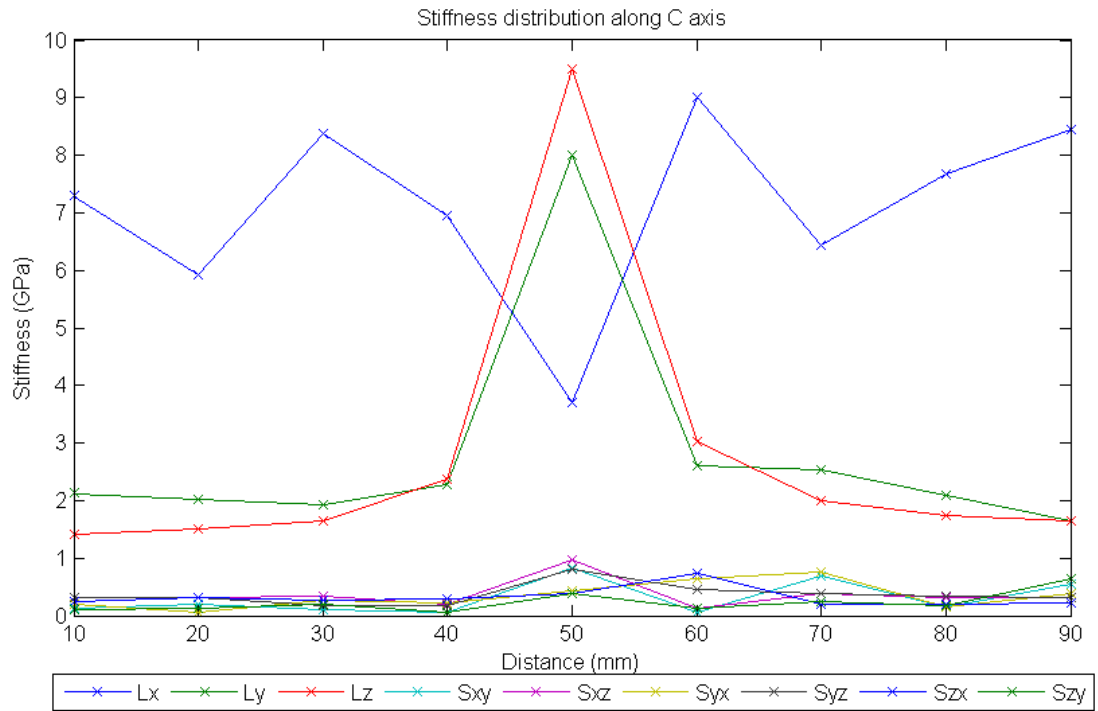


Figure 7.17: Stiffness distribution along C axis

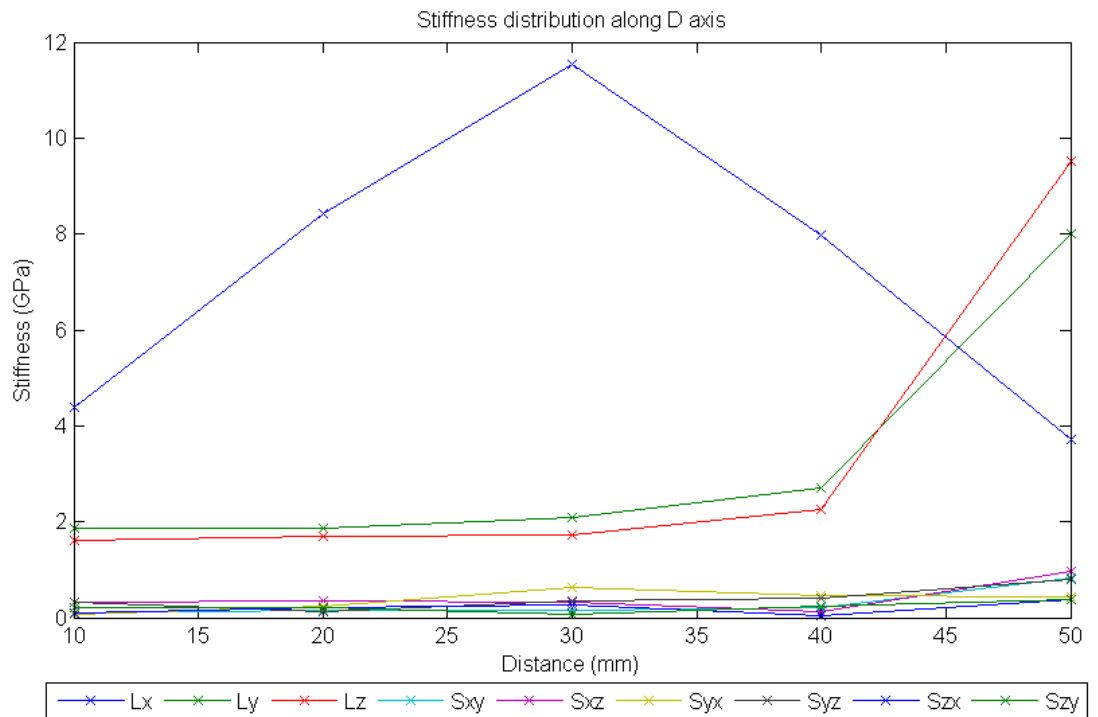


Figure 7.18: Stiffness distribution along D axis

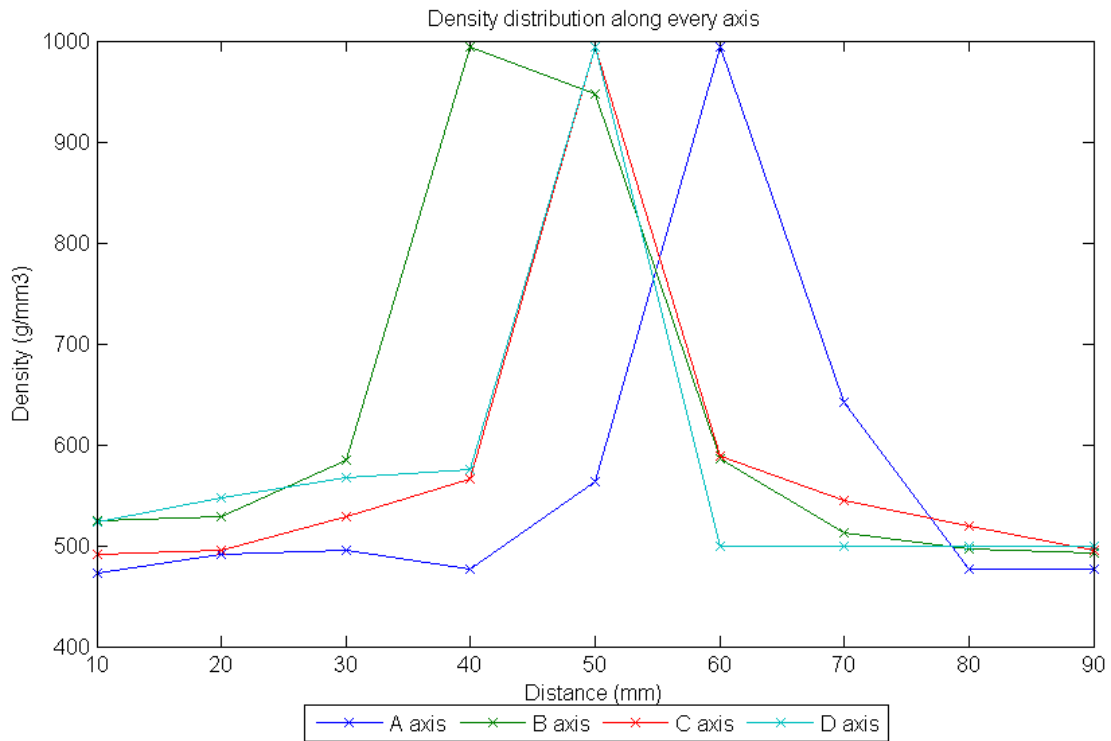


Figure 7.19: Density distribution along axis

In plotted graphs stiffness of longitudinal X,Y,Z directions for every axis are shown. Starting from +A axis it can be observed that stiffness is decreasing in X direction as it is approaching knot area and for Y and Z directions stiffness increasing. Direction of the grain changing its angle approaching to the knot and it becomes perpendicular to the former direction. Same effect is observed in -A axis where stiffness in X direction is decreasing and stiffness in Z,Y direction is increasing. For technological reason it was not possible to evaluate +B axis, but in -B axis same principle of stiffness distribution as it is in A axis is observed. In both +C and -C axis rise of stiffness is observed as it is approaching knot area. Specimen “10” should be mentioned separately as it consists of both knotted and plain timber in the same specimen. Density of such specimen is about twice bigger than average density of the set that could be one of the reasons why such high stiffness properties are obtained after evaluation. For D axis which is symmetrical to C axis, obtained stiffness properties in the X direction is 20% smaller. It seems that stiffness properties in Z and Y directions remain unchanged as evaluated specimens consist only from plain timber without inhomogeneities. In the area of the knot stiffness in X direction is decreasing and in the Y and Z direction is increasing.

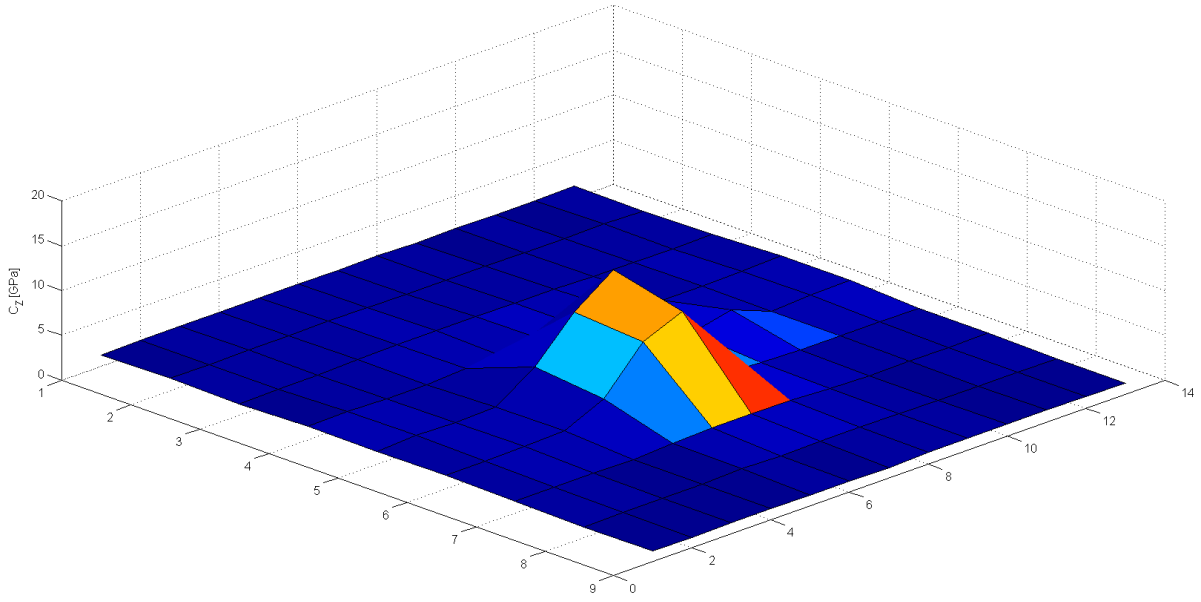


Figure 7.20:Second sample longitudinal stiffness distribution along Z direction

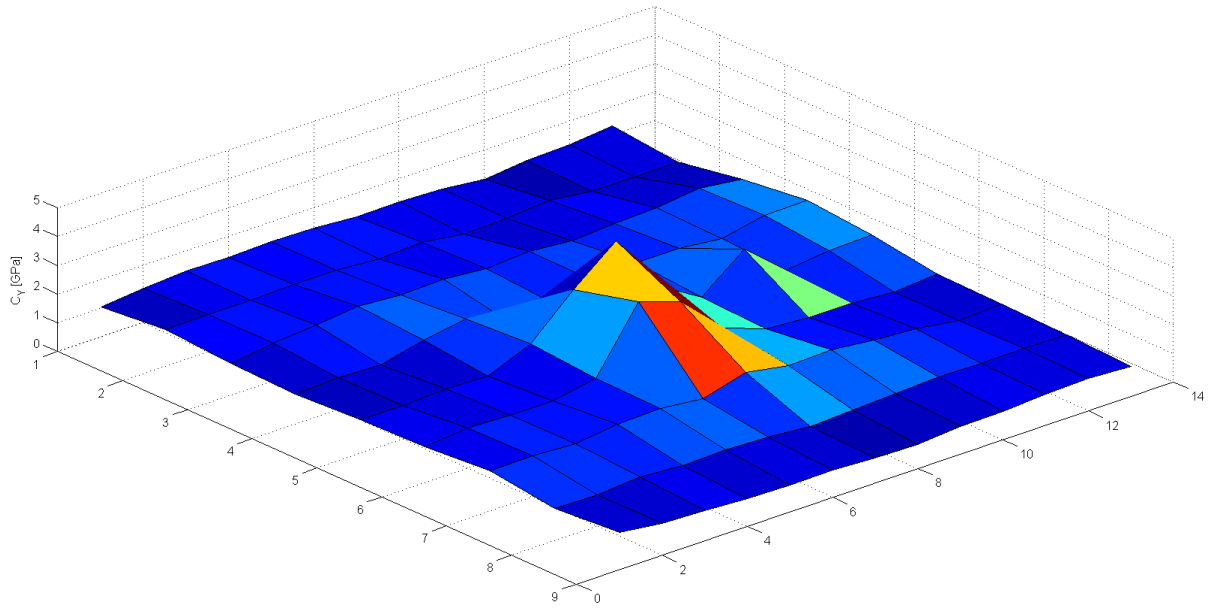


Figure 7.21:Second sample longitudinal stiffness distribution along Y direction

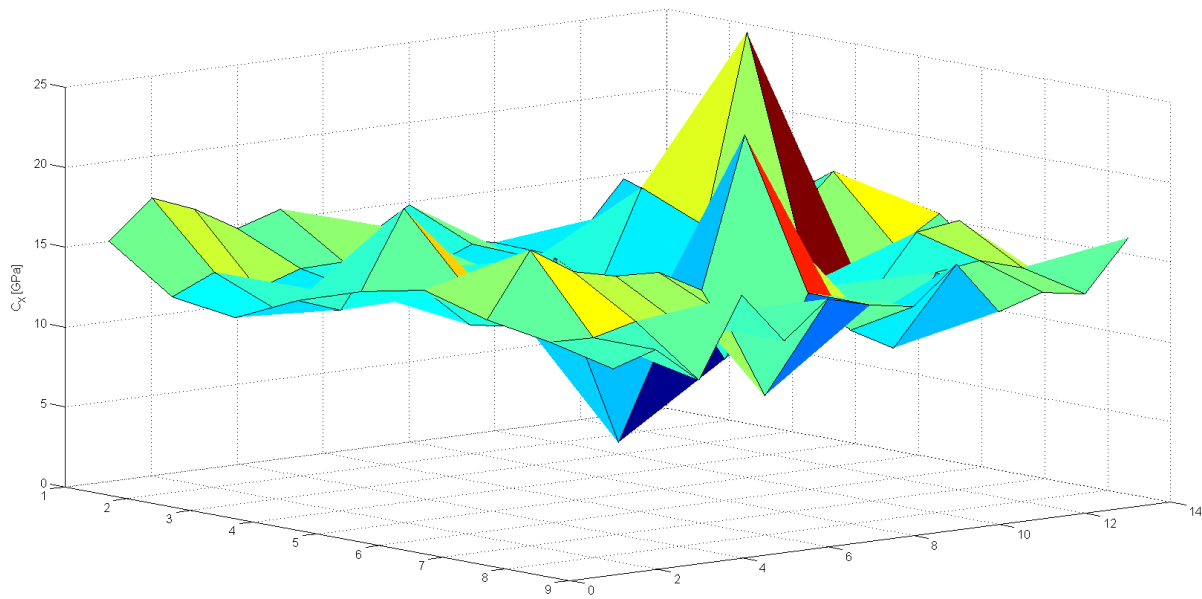


Figure 7.22:Second sample longitudinal stiffness distribution along X direction

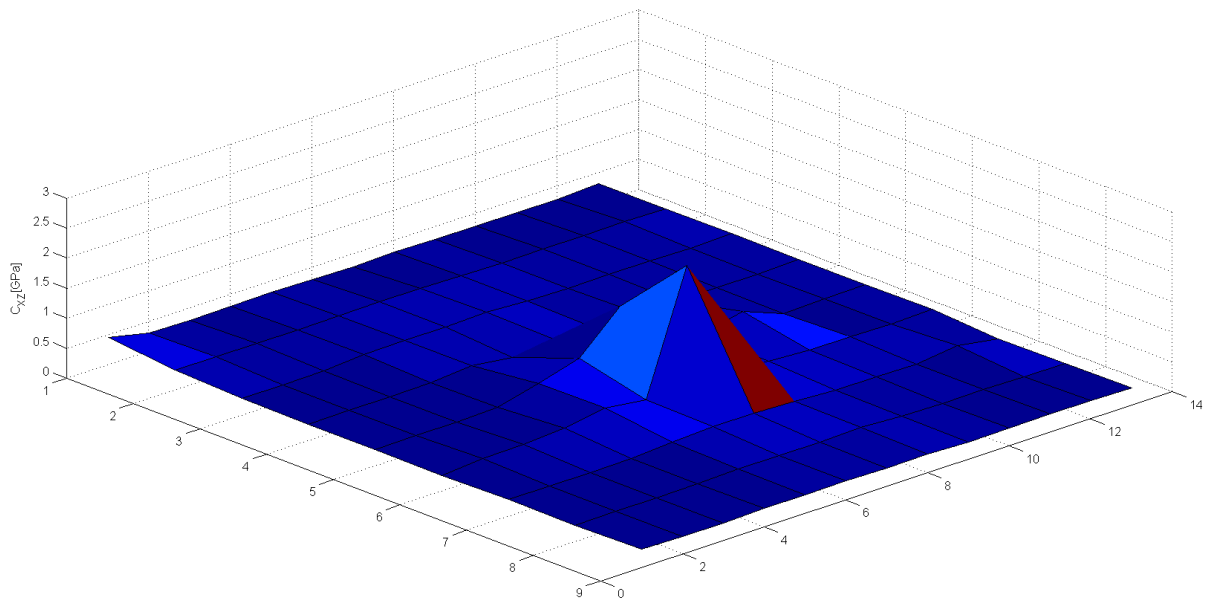


Figure 7.23:Second sample shear stiffness distribution along XZ direction

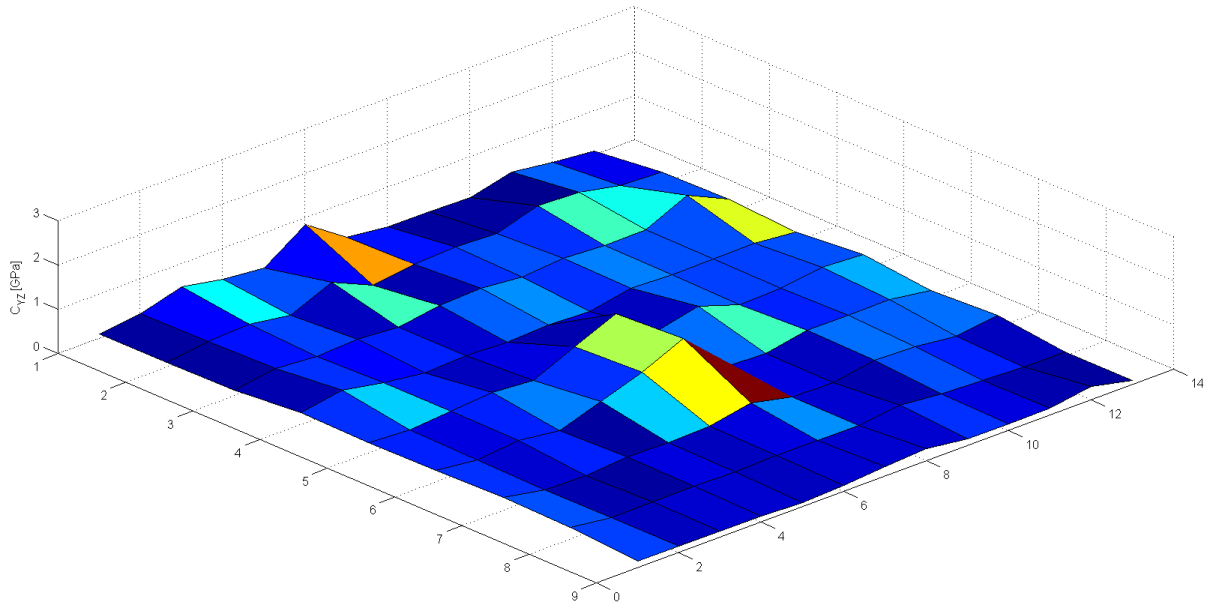


Figure 7.24:Second sample shear stiffness distribution along YZ direction

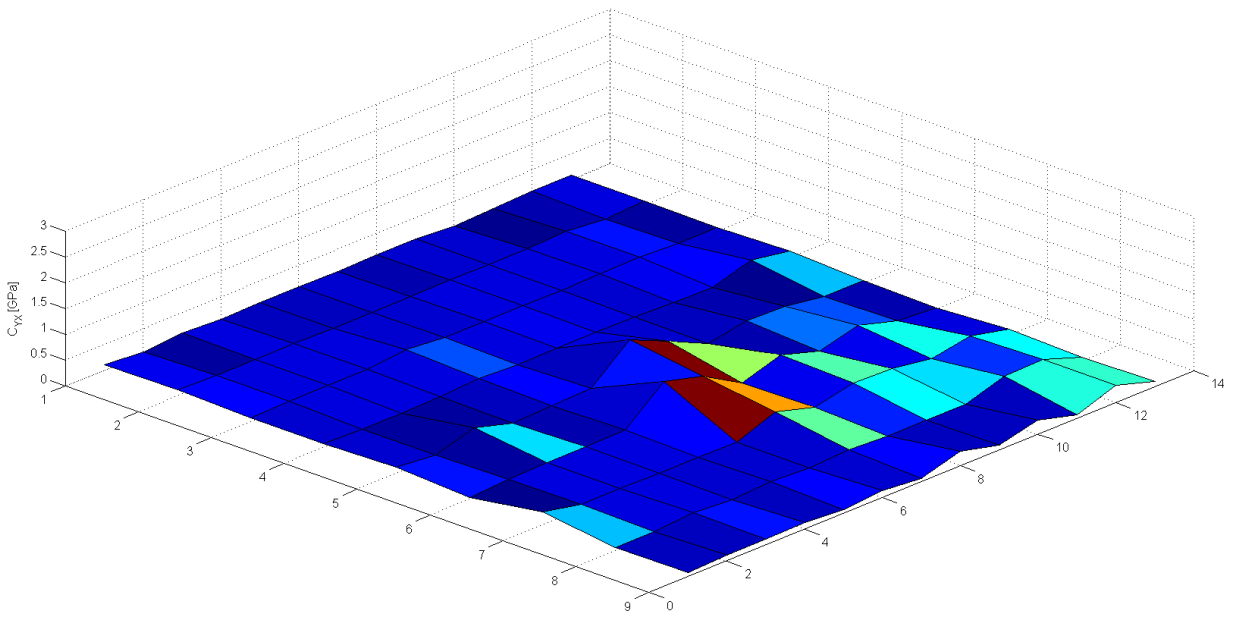


Figure 7.25:Second sample shear stiffness distribution along YX direction

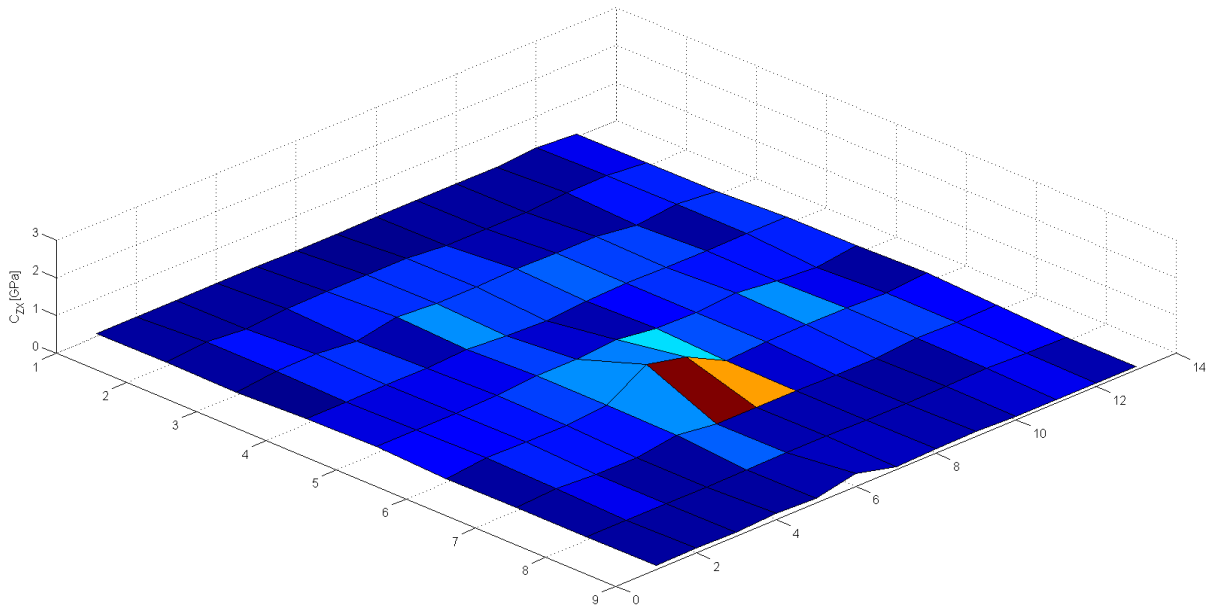


Figure 7.26: Second sample shear stiffness distribution along ZX direction

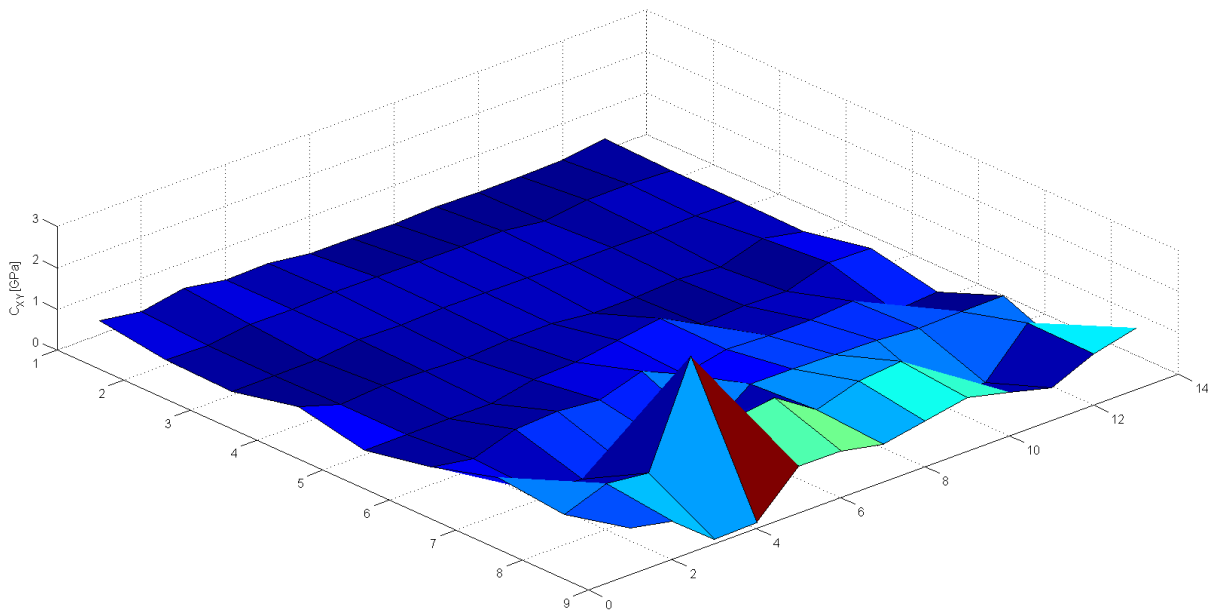


Figure 7.27: Second sample shear stiffness distribution along XY direction

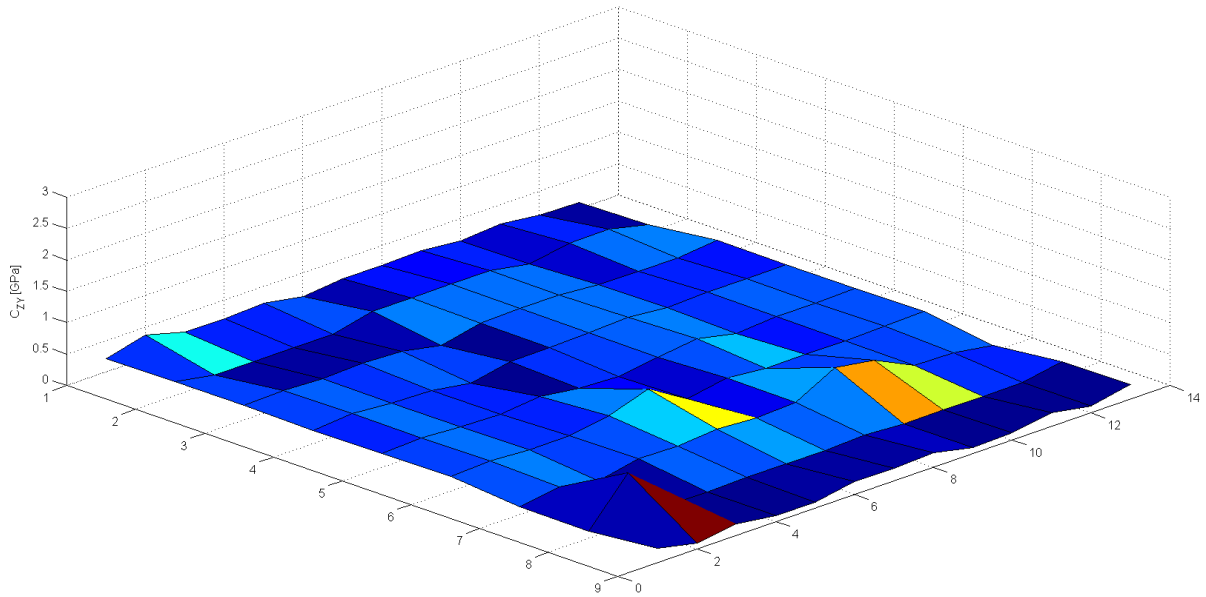


Figure 7.28: Second sample shear stiffness distribution along ZY direction

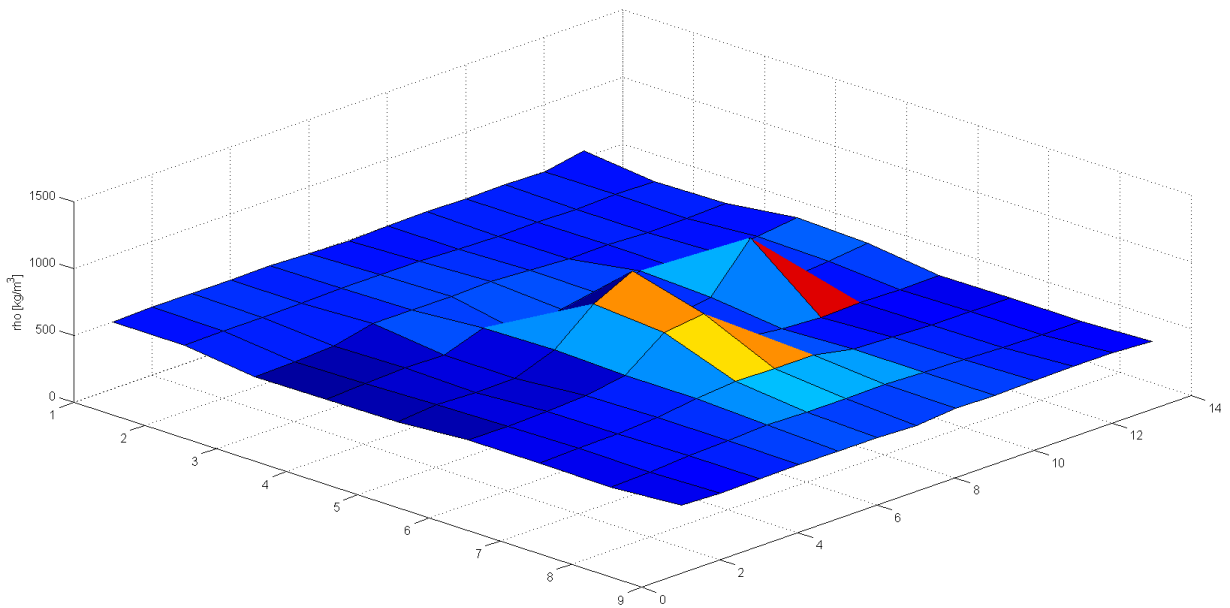


Figure 7.29: Second sample density distribution

Looking at the second example it is observed that places around knot is characterized with the highest stiffness. It is observed along Y direction the same as it was observed in first example. Except the region around of the knot stiffness is rather average as it is same where distribution of density in the knot region is higher than in plain timber. Stiffness distribution in knot region can be explained by higher of density of knot and change of wood fiber direction that perpendicular to plain timber.

8. Conclusions

- In this master thesis inhomogeneous anisotropic material was investigated using non-destructive technique with ultrasound. Using non – destructive evaluation methods physical properties was investigated in longitudinal, tangential and radial directions. For samples Norway spruce (*Picea abies(L.) Karst*) was used. For better wood understanding two samples were used. The first sample was cut that the knot area was in the center of the specimen axis. The wood around the knot was cut into horizontal, vertical and sidelong directions with angle of 45° between horizontal (A) and vertical (B) axis (**Figure 7.15-18**).
- Before measurements all specimens were marked, measured and weighted. Density was calculated for plain and knotted timber where average density of Norway spruce (*Picea abies(L.) Karst*) was about 500 kg/m³ and for knotted density was between 800kg/m³ and 900 kg/m³.
- Specimens were formed from sample consisting from plain timber and knotted timber in the center. During research part it was possible to answer question how much physical and stiffness properties differentiate in both types of wood.
- Was noticed that knot is growing perpendicular to the wood grain and have different structure. Looking at the knot region it is not possible to notice layers of *Earlywood* and *Latewood* as it is noticed in the plain timber. Knot region can be described as single system with its own growing rings and altered structure. Although, porosity in this master thesis was not investigated, it can be stated that voids of empty spaces will be much lower in knotted timber than it is in plain timber.
- After main physical properties were measured evaluation with non-destructive methods using ultrasound started. For every specimen's in both samples, three longitudinal and six transversal measurements were taken. Using generalized Hook's law stiffness for every specimen longitudinal and shear components was calculated getting results in GPa and representing them graphically (**Figure 7.22-29**).
- In this master thesis one of the objective was investigated how stiffness changing around and approaching knot region. From given samples it was possible to take specimens that consist of knotted wood and investigated them using non-destructive technology. First sample stiffness in longitudinal (Lx) direction approaching the knot is decreasing and stiffness in tangential (Ly) and radial (Lz) direction is increasing, same affect is observed in all directions in the first sample.
- It is known that mechanical properties of in the radial direction are much higher than in the tangential direction, and both radial and tangential properties are about one order of magnitude lower than in the longitudinal direction. This fact depends from the cell shape in the cross-section

plane which consists of irregular hexagonal cell which causes the anisotropy in the transverse plane and, also by the effect of rays in the radial direction.

- The theory for solid orthotropic materials shows that the following relationship for transversal waves is not valid: $c_{LR} \neq c_{RL}$; $c_{LT} \neq c_{TL}$; $c_{TR} \neq c_{RT}$. In the case of wood is not exactly the same because wood is an organic body and has a more complex structure, also fiber angle is changing critically reaching area of the knot (**Figure: 8.1**). These is partially because for small samples there are too many reflections on the wood walls and the transversal signals are not clear and are complemented with longitudinal signals.
- Mathematical model described in Section 5 enables to compute mechanical properties for anisotropic materials. Using Hooke's law is possible to find small displacements caused by ultrasound vibrations. Elastic properties as average volume of stress are defined by average volume of the strains and elastic constants. Knowing materials Lamé parameters (λ and μ) is possible to derive Young's modulus, shear modulus and Poisson's ratio and calculate materials mechanical properties. Described mathematical model can be used as alternative way to check validity of results.

9. References list

Aicher, S., Dill-Langer, D. **Influence of cylindrical anisotropy of wood and loading conditions on off-axis stiffness and stresses of a board in tension perpendicular to the grain.** *Otto Graf Journal*, (1996) 7:216–242p.

Aira J. R., Francisco Arriaga, Guillermo Iniguez-Gonzalez 2014. **Determination of the elastic constants of Scots pine (*Pinus sylvestris* L.) wood by means of compression tests.** *Biosystems Engineering* 126 (2014) 12 – 22 p.

Aiskila S., Saranpää P., Fagerstedt K., Laakso T., Löija M., Mahlberg R., Paajanen L. and Ritschkoff A.C. **Growth Rate and Wood Properties of Norway Spruce Cutting Clones on Different Sites.** *Silva Fennica* 40(2) (2005); 247-225p.

Ban V., Arriaga F., Guaita M.. **Determination of the influence of size and position of knots on load capacity and stress distribution in timber beams of *Pinus sylvestris* using finite element model.** *Biosystems Engineering* 114 (2013) 214 – 222p.

Bano V., Arriaga F., Soila A., Guaita M. **Prediction of bending load capacity of timber beams using a finite element method simulation of knots and grain deviation.** *Biosystems Engineering* 109 (2011) 241 – 249 p.

Bao, J., (2003). **Lamb waves generation and detection with piezoelectric wafer active sensors.** *Beijing Univerisyt of Aeronautics and Astronautics.*

Baradit, E, Keunecke, D, Schnider T, Niemz, P. **Stiffness Moduli of Various Extraneous Species Determined with Ultrasound.** (2012) *Wood Research* 57(1):2012 173-178p.

Barnett, J.R., Chaffey, N.J., Barlow, P.W.,. In: Butterfield, B.G. **Cortical microtubules and microfibril angle.** (Ed.), *Proceedings of the IAWA/IUFRO International Workshop on the Significance of Microfibril Angle to Wood Quality.* Westport, New Zealand, (1997) pp. 253–271p.

Berryman J. G.. **Mechanics of layered anisotropic poroelastic media with applications to effective stress for fluid permeability** *International Journal of Engineering Science* 49 (2001) 122-139p.

Birgul, B., (2009). **Hilbert transformations of waveforms to determine shear wave velocity in concrete.** *Cement and concrete Reserach* 39 (2009) 696-700p.

Bodig, J. **The effect of anatomy on the initial stress-strain relationship in transverse compression.** *Forest Products J.*, (1965) 15:197–202p.

Borst K., Bader T. K., Wikete C.. **Microstructure–stiffness relationships of ten European and tropical hardwood species.** *Journal of Structural Biology* 177 (2012) 532 – 542 p.

Brekhovskikh L.M.. **Waves in Layered Media.** (1981) *Academic Press, New York.*

Cai, Z., Ross R. **Mechanical Properties of Wood-Bases Composite Materials.** *General Technical Report FPL-GTR-19*, 2006, 12p.

Casadei F., Rimoli J.J 2013. **Anisotropy-induced broadband stress wave steering in periodic lattice.** *International Journal of Solids and Structures* 50 (2013) 1402 – 1414p.

Christoffel EB (1877). **Ueber die Fortflanyung von Stößen durch elastische fest Körper.** *Annali di Matematic* 8:193-243p.

Copenheaver A., Elizabeth A. Pokorski , Joseph E. Currie , Marc D. Abrams. **Causation of false ring formation in *Pinus banksiana*: A comparison of age, canopy class, climate and growth rate Carolyn.** *Forest Ecology and Management* 236 (2006) 348 – 355p.

Crampin, S., (1981) **A review of wave motion in anisotropic and cracked elastic media.** *Wave Motion* , 3 343–391p.

Cretu N., Delsanto P.P., Nita G., Rosca C., Scalerandi M., Sturzu I., , Acoust J.. **Propagation of acoustic pulses in inhomogeneous 1-D media.** *Soc. Am.* 104 (1998) 57– 63p.

Cretu N., Nita G.. **Pulse propagation in finite elastic inhomogeneous media.** *Computational Material Science* 31 (2004) 329-336p.

D'arrigo R. D., Malmstrom C. M., Jacoby G. C., S. O. Los and D. E. Bunker. **Correlation between maximum latewood density of annual tree rings and NDVI based estimates of forest productivity.** *Int. J. Remote Sensing* (2000), 2329-233p.

Diaz C. A., Afrifah K. A. , Jin S, Matuana L. M.. **Estimation of modulus of elasticity of plastics and wood plastic composites using a Taber stiffness tester.** *Composite Science and Technology* 71 (2011) 67-70 p.

Fellah, Z., Fellah, M., Depollier, C., (2013). **Transient Acoustic Wave Propagation in Porous Media.** *Fellah et al.*, 1-34p.

Green D. W., Winandy J. E. and David E. **Mechanical Properties of Wood.** Kretschmann *Forest Products Laboratory. Wood handbook—Wood as an engineering material.* (1999), 1-46p.

Green, G., (1839). **On the propagation of light in crystallized media.** *Trans Cambridge Philos Soc* 7(2):121-140p.

Guindos P., Ortiz J.. **The utility of low-cost photogrammetry for stiffness analysis and finite-element validation of wood with knots in bending.** *Biosystems Engineering* 114 (2013) 86 – 96 p.

Haines D.W., Leban J.M., Herbe C, **Determination of Young's modulus for spruce, fir and isotropic materials by the resonance flexure method with comparisons to static flexure and other dynamic methods.** *Wood Science and Technology* 30 (1996) Springer –Verlag 1996

Hoffmeyer, P., Damkilde, L., Pedersen, T. N. **Structural timber and glulam in compression perpendicular to grain.** *Holz als Roh - und Werkstoff*, (2000) 58:73–80p.

Hofstetter K., and Kristofer E.G., **Hierarchical modelling of microstructural effects on mechanical properties of wood. A review.** *Holzforschung*, Vol. 63 (2009); 130-138p.

Hofstetter K., Hellmich C., Eberhardsteiner J. **Development and experimental validation of a continuum micromechanics model for the elasticity of wood.** *European Journal of Mechanics A/Solids* 24 (2005) 1030-1053 p.

Jäger A., Th. Bader, K. Hofstetter, J. Eberhardsteiner. **The relation between indentation modulus, microfibril angle, and elastic properties of wood cell walls.** *Composites: Part A* 42 (2011) 677–685p.

Jenkel C., Kaliske M. **Finite element analysis of timber containing branches – An approach to model the grain course and the influence on the structural behavior.** *Engineering Structures* 75 (2014) 237 – 247 p.

Joffre T., Cristian Neagu R., Gamstedt E. K. **Modelling of the hygroelastic behaviour of normal and compression wood tracheids.** *Journal of Structure Biology* 185 (2014) 89-98 p.

Johansson E., Johansson D., Skog J., Fredriksson M.. **Automated knot detection for high speed computed tomography on *Pinus sylvestris* L. and *Picea abies*(L.) Karst. using ellipse fitting in concentric surfaces.** *Computers and Electronics in Agriculture* 96 (2013) 238 – 245 p.

Jongmans D., Demanet D., **The importance of surface waves in vibration study and the use of Rayleigh waves for estimating the dynamic characteristics of soils,** *Eng. Geol.* 34 (1993) 105–113.

Kennedy, R. W. **Wood in transverse compression.** *Forest Prod. J.,* (1968) 18:36–40p.

Klungness J.H., Ahmed A, Ross-Sutherland N, AbuBakr S. **Lightweight, high capacity paper by fiber loading: filler comparison.** *Nord Pulp Pap Res J* (2000);15(5):345–50p.

Kohlhauser C., Hellmich C., **Determination of Poisson's ratios in isotropic, transversely isotropic, and orthotropic materials by means of combined ultrasonic-mechanical testing of normal stiffnesses: Application to metals and wood.** *European Journal of Mechanics A/Solids* 33 (2012) 82-98p.

Kohlhauser C., Hellmich C.. **Ultrasonic contact pulse transmission for elastic wave velocity and stiffness determination: Influence of specimen geometry and porosity.** *Engineering Structures* 47 (2013) 115 – 133 p.

Krähenbühl A., Kerautret B., Debled I. R., Mothe F. , Longuetaud F. **Knot segmentation in 3D CT images of wet wood.** *Pattern Recognition* 47 (2014) 3852 – 3869p.

- Krautkrämer J., Krautkrämer, H., **Werkstoffprüfung mit Ultraschall.**(1986)Berlin, Springer,708 p.
- Lane, C. (2014). **The Development of a 2D Ultrasonic Array Inspection for Single Crystal Turbine Blades.** Springer, 2014, IX, 133p. 80 illius.
- Lawrence W. Braile, **Seismic Waves and the Slinky: A Guide for Teacher.** (2010) Department of Earth and Atmospheric Sciences, 1-40p.
- Leisk G.G., Saigal A., **Digital computer algorithms to calculate ultrasonic wave speed, Mater. Eval. 54 (7) (1996) 840–843p.**
- Lindstrom, H., Evans, J.M., Verrill, S.P. **Influence of cambial age and growth conditions on microfibril angle in young Norway spruce (*Picea abies*[L]. Karst.). Holzforschung 52 (1998)., 573–581p.**
- Liu E., Chapman M., Zhang Z., John H. Queen. **Frequency-dependent anisotropy: Effects of multiple fracture sets on shear-wave polarizations.** *Wave Motion* 44 (2006) 44 – 57p.
- Love, A.E.H., (1994). **A treatise on the mathematical theory of elasticity, 4th edn.** Dover publications, New York.
- Machado J. S., Louzada J. L., Nunes L., Anjos O., Rodrigues J., Simões R. M.S., Pereira H.. **Variation of wood density and mechanical properties of blackwood (*Acacia melanoxylon*R. Br.).** *Materials and Design* 56 (2014) 975 – 980 p.
- Mason,W, Thurston, R.N. **Physical Acoustics Volume XV.** Academic Press, Inc, 1981,380p.
- Mishnaevsky L. Jr., Hai Qin. **Micromechanical modelling of mechanical behaviour and strength of wood: State-of-the-art review.** *Computational Materials Science* 44 (2008) 363 – 370 p.
- Moberg L.. **Models of internal knot properties for *Picea abies*.** *Forest Ecology and Management* 147 (2001) 12 – 138 p.

Morales Conde M.J., Rodríguez C. Li, Rubio de Hita P.. **Use of ultrasound as a nondestructive evaluation technique for sustainable interventions on wooden structures.** *Building and Environment* 82 (2014) 247 – 257 p.

Nairn, J.A. **A Numerical Study of the Transverse Modulus of Wood as a Function of Grain Orientation and Properties** (2006) *Holzforschung*, in press.

Ogam E., Wirgin A., Schneider S., Fellah Z.E.A., Xu Y. **Recovery of elastic parameters of cellular materials by inversion of vibrational data.** *Journal of Sound and Vibration* 313 (2008) 525 – 543p.

Picotti S., Carcione J. M., Santos J. E. **Oscillatory numerical experiments in finely layered anisotropic viscoelastic media.** *Computer & Geosciences* 43 (2012) 83 – 89p.

Plomion, Ch., Leprovost, G., Stokes. **Wood formation in trees.** *A. Plant Physiology*, (2001). 127, 1513–1523p.

Potel C. , Belleval J. F., and Gargou Y. **Floquet waves and classical plane waves in an anisotropic periodically multilayered medium: Application to the validity domain of homogenization.** *URA CNRS 1505,(1995) Universite de Technologie de Compiègne, BP 649, 60206 Compiègne Cedex, France*

Price, A. T. **A mathematical discussion on the structure of wood in relation to its elastic properties.** *Philosophical Transactions of the Royal Society of London.* (1929) *Series A*, 228:1–62p.

Qing H., Mishnaevsky L. Jr. **3D hierarchical computational model of wood as a cellular material with fibril reinforced, heterogeneous multiple layers.** *Mechanics of Materials* 41 (2009) 1034 – 1049 p.

Raven, Peter H.; Evert, Ray F.; Curtis, Helena. **Biology of Plants.** *New York, N.Y.: Worth Publishers,* (1981), 641p.

Reiterer A., G. Sinn, S.E. Stanzl-Tschegg. **Micromechanics of Wood: state-of-the-art review** *Mater. Sci. Eng. A—Struct.* 332 (2002) 29–36p.

Reynolds T., Harris R., Chang W. S. **Stiffness of dowel-type timber connections under pre-yield oscillating loads.** *Engineering Structures* 65 (2014)21-29 p.

Rokhlin S.I., Wang L.. **Ultrasonic waves in layered anisotropic media: characterization of multidirectional composites** *International Journal of Solids and Structures* 39 (2002) 4133 – 4149p.

Saavedra Flores E.I., DiazDela F.A., Friswell M.I., Ajaj R.M.. **Investigation on the extensibility of the wood cell-wall composite by an approach based on homogenisation and uncertainty analysis.** *Composite Structures* 108 (2014) 212 – 222 p.

Saavedra Flores E.I., Souza E.A., Pearce C., **A large strain computational multi-scale model for the dissipative behavior of wood cell-wall.** *Computational Materials Science* 50 (2011) 1202 – 1211 p.

Saavedra Flores E.I., Friswell M.I. **Multi-scale finite element model for a new material inspired by the mechanics and structure of wood cell-walls.** *Journal of the Mechanics and Physics of Solids* 60 (2012) 1296 – 1309p.

Scalerandi M., Cretu N., Chiriacescu S.T., Sturzu I., Rosca C., in: Brebia C.A. (Ed.). **Computational Acoustics and its Environmental Applications, vol. II, Computational Mechanics Publications, Southamton-Boston.** (1997), pp. 161–168p.

Schellekens J.C.J., Borst R.. **The use of the Hoffman yield criterion in finite element analysis of anisotropic composites.** *Computers & Structures* Vol. 37, No. 6, pp. (1990), 1087 – 1096p.

Shipsa, A., Berglund, L. A. **Shear coupling effect on stress and strain distributions in wood subjected to transverse compression.** *Composites Science and Technology*, (2006) in press.

Singh A. P. , Anderson R. , Park B. D. , Nuryawan A.. **A novel approach for FE-SEM imaging of wood-matrix polymer interface in a biocomposite.** *Micron* 54 -55 (2013) 87 – 90 p.

Suvi P. Pohjamo, Jarl E. Hemming, Stefan M. Willför, Markku H.T. Reunanen, Bjarne R. Holmbom. **Phenolic extractives in Salix caprea wood and knots.** *Phytochemistry* (2003) 165 – 169p.

Tabiei A. , Wu J.. **Three-dimensional nonlinear orthotropic finite element material model for wood.** *Composite Structures* 50 (2000) 143 – 149 p.

Timell, T.E. **Compression Wood in Gymnosperms.** Vol 2. *Springer-Verlag, Heidelberg, (1986)* 983–1262p.

Tulika M., Rusin A.. **Microfibril angle in wood of Scots pine trees (*Pinus sylvestris*) after irradiation from the Chernobyl nuclear reactor accident.** *Environmental Pollution* 134 (2005) 195–199p.

Walker J.S., Gathright J.. **Exploring one-dimensional quantum mechanics with transfer matrices.** *Am. J. Phys.* 62 (1994) 408–422p.

Willis M.E., Toksöz M.N., **Automatic P and S velocity determination from full waveform digital acoustic logs,** *Geophysics* 48 (12) (1983) 1631–1644p.

Zhang Z., Wang G., Harris J. M. **Multi-component wavefield simulation in viscous extensively dilatancy anisotropic media.** . *Physics of the Earth and Planetary Interiors* 114 (1999) 25-38p.

Zhao J., Zhao X.B., Cai J.G.. **A further study of P-wave attenuation across parallel fractures with linear deformational behavior.** *International Journal of Rock Mechanics & Mining Sciences* 43 (2006) 776-788p.